DEC 23 1946

ARR No. E6A07

NATIONAL ADVISORY COMMITTEE FOR AERONAUTICS

WARTIME REPORT

ORIGINALLY ISSUED

January 1946 as
Advance Restricted Report E6A07

DETERMINATION OF GAS TEMPERATURES FROM THE FREQUENCY OF KNOCK-INDUCED GAS VIBRATIONS IN AN INTERNAL-COMBUSTION ENGINE

By W. E. Moeckel and J. C. Evvard

Aircraft Engine Research Laboratory
Cleveland, Ohio

NACA

WASHINGTON

E-132

NATIONAL ADVISORY COMMITTEE FOR AERONAUTICS

ADVANCE RESTRICTED REPORT

DETERMINATION OF GAS TEMPERATURES FROM THE FREQUENCY OF KNOCK-INDUCED GAS VIBRATIONS IN AN INTERNAL-COMBUSTION ENGINE

By W. E. Moeckel and J. C. Evvard

SUMMARY

Object. - To develop a method of obtaining gas temperatures from the frequency of knock-induced gas vibrations in an internal-combustion engine cylinder.

Scope. - Measurements were made of the frequency of knock-induced gas vibrations in a CFR cylinder. The variation of this frequency with fuel-air ratio, inlet-air temperature, and spark advance was determined. Comparisons were also made of frequencies obtained using a shrouded and an unshrouded intake valve and of frequencies obtained when the charge was fired only on alternate engine cycles. In obtaining temperatures from the frequency data, the gas-vibration waves were assumed to be propagated at sonic velocity. The composition of the products of combustion and the ratio of specific heats of those products were computed as functions of fuel-air ratio and temperature, and the resulting data were used in calculating temperatures from frequency data. The frequency-derived temperatures were compared with temperatures calculated from pressure data, with temperatures obtained from thermodynamic charts, with temperatures indicated by a thermal plug placed in a spark-plug hole, and with temperatures obtained by the spectral-line reversal method by other investigators.

Summary of results. - The results of this investigation may be summarized as follows:

1. Temperatures calculated from frequency data were in agreement with temperatures measured by the spectral line-reversal method in previous investigations and were about 700° F lower than temperatures obtained from thermodynamic charts. Temperatures obtained from peak-pressure data were found to be in poor agreement with frequency-derived temperatures.

2. A maximum error of only about 3.5 percent would be introduced in temperatures calculated from frequency data if the variation of the ratio of specific heats with fuel-air ratio and temperature were neglected.

3. A maximum error of about 14 percent would be introduced in frequency-derived temperatures if the variation of molecular weight with fuel-air ratio were neglected. The variation of molecular weight with temperature, however, is less than 2 percent between 2500° and 5000° F.

INTRODUCTION

Despite extensive research in the field of knocking combustion, the determination of the variation of the frequency of knock-induced cylinder gas vibrations with engine conditions has received little attention. As a new approach to such problems as the determination of cylinder gas temperatures and heat transfer during the working cycle, the measurement of gas-vibration frequencies has many interesting and potentially valuable possibilities. It has an advantage over other experimental methods in that measurements may be made under many operating conditions with little special or complex equipment. The interpretation of vibration-frequency data will not, of course, be entirely satisfactory until an adequate theory of cylinder gas vibrations has been formulated and its validity checked with sufficient experimental data. The present assumption that the vibration waves are propagated at equilibrium sonic velocity is obviously not completely satisfactory. It is known that sound velocity is influenced by the dissociation and recombination reactions taking place in the cylinder gases during the period in which vibrations occur. (See reference 1.) It is also recognized that the phenomenon of heat-capacity lag (see reference 2) may influence sound propagation. Experimental evidence reported in references 3 and 4, however, seems to indicate that to a good approximation the vibration waves following knock are propagated at equilibrium sonic velocity and that the portion of the gases involved in dissociation and recombination reactions during the period of gas vibration is almost negligibly small.

An examination of high-speed motion pictures of knocking cycles by C. D. Miller of this laboratory indicated that the shock wave associated with knock is initially propagated at supersonic speed. The speed of this initial shock wave during its first traversal of the combustion chamber was, however, found on analysis to average about 3000 feet per second (see reference 5), whereas a rough estimate of the velocity of sound, made on the basis of calculations presented in the present report, gives a value of about 3160 feet per second, which indicates that the initial shock is propagated at supersonic speed for only a portion of the first traversal of the chamber.

Experiments to determine the frequency and the duration of combustion noises in a bomb and in an engine cylinder were reported by Wawrziniok (reference 3) in 1933. The author recognized that "the noise is a secondary phenomenon of the gas vibrations in the bomb" and that the frequency of the vibrations depended upon the temperature of the gases and the dimensions of the combustion chamber.

In 1934, C. S. Draper (reference 4) published a report containing a theoretical analysis, based upon the wave equation, of the possible modes of gas vibration in a cylindrical chamber together with experimental data on the frequency of gas vibrations in an engine cylinder. Theoretical frequencies were calculated for the assumed modes of vibrations from the equilibrium sound-velocity equation: the pressures and the densities were obtained from pressure cards and from fuel-flow and air-flow measurements, respectively. The gas vibrations were recorded by a photographic oscillograph. Gas vibrations were induced both by explosion of pistol primers and by knock. The measured frequencies agreed closely with the calculated values.

In the present investigation the variation with fuel-air ratio of the frequency of gas vibrations under knocking conditions has been determined for several engine conditions. Temperatures have been calculated from these frequencies and are compared with temperatures calculated from pressure data, from thermodynamic charts, and from reports of investigators who used the spectral-line reversal method.

THEORY

In the calculation of gas temperatures from gas-vibration frequencies, the equilibrium sound-velocity equation was combined with the equation giving the possible frequencies of vibration of gases in a flat-end cylinder (see reference 4):

$$n = c\left[\frac{(\beta a)^2}{(2\pi a)^2} + \frac{g^2}{4h^2}\right]^{1/2} \qquad (1)$$

$$c = (\gamma RT/M)^{1/2} \qquad (2)$$

where

n	frequency, cycles per second
c	speed of propagation, feet per second
a	radius of cylinder, feet
(βa)	roots of $\left[dJ_s(\beta r)/dr\right]_{r=a} = 0 \quad s = 0, 1, 2, \ldots$
J_s	Bessel's function of first kind and sth order
r	distance from center of cylinder
g	0, 1, 2, . . .
h	height of cylinder chamber, feet
γ	ratio of specific heats
R	gas constant, 4.973×10^4 foot-poundals per mole per $^{\circ}R$
T	absolute temperature, $^{\circ}R$
M	molecular weight of cylinder charge

(A refinement of equation (2) for nonperfect gases is presented in appendix A.)

At the temperatures existing during the period of knock-induced gas vibrations only one mode of vibration in the CFR cylinder yields frequencies below 10,000 cycles per second. This mode is also the one that would be expected to be most readily excited by knock; that is, one having a single nodal pressure plane at the diameter perpendicular to the diameter through the center of the position where knock occurs. (See fig. 3(a), reference 4.) For this mode of vibration, $g = 0$ and $(\beta a) = 1.841$; equation (1) then becomes:

$$n = c(1.841)/2\pi a \qquad (3)$$

When equations (2) and (3) are combined, there is obtained:

$$\frac{\gamma T}{M} = \frac{4\pi^2 a^2 n^2}{(1.841)^2 \ (4.973 \times 10^4)} = kn^2 \tag{4}$$

For the CFR cylinder used in these tests, $a = 0.1354$ foot; consequently $k = 4.297 \times 10^{-6}$ mole-seconds^2 $^{\circ}$R per pound.

Because γ and M vary with the temperature and the composition of the cylinder charge, it is necessary to evaluate them as functions of temperature for several fuel-air ratios with considerable accuracy in order to be able to determine the temperatures from equation (4). Since no data of sufficient accuracy were available on the mixture of gases composing the products of combustion in the temperature range of interest, the required values of γ and M were calculated from specific-heat data and from the equilibrium reactions of the constituent gases. The percentage composition of the products of combustion for several fuel-air ratios was first calculated by the method given in reference 6 and the specific heats were then weighted according to these calculated percentages. An exposition of these calculations, together with the references from which the basic data were obtained, is given in appendix B. The results of these calculations are summarized in figures 1 and 2 and in tables I and II. The specific heats at zero pressure c_p^o, which were used in the calculations, are plotted against temperature in figure 3. An inspection of table II and equation (4) shows that the maximum error in temperatures calculated from frequencies would be about 3.5 percent if the variation of γ with temperature and fuel-air ratio were neglected and about 14 percent if M were considered constant with respect to fuel-air ratio and temperature.

The relation between the four variables — fuel-air ratio, temperature, frequency, and γ — obtained by the calculations is presented in figure 4. The nature of the relations between the variables indicates that the frequency-averaged temperature will be slightly lower than the average gas temperature. Since the frequency-temperature relation at constant fuel-air ratio was almost linear, the error thus introduced was negligible.

DESCRIPTION OF APPARATUS AND TEST PROCEDURE

A supercharged CFR engine was used for all tests. It was equipped with a cylinder having three horizontal spark-plug holes and an auxiliary hole located at the top and slanted at 25° to the vertical. Dual ignition was used for all tests, and a shrouded intake valve was used for part of them to improve the reproducibility of knocking cycles. A schematic diagram of the cylinder, showing the location of the spark plugs and the position of the shroud, is presented in figure 5.

The following engine conditions were maintained during the tests:

Engine speed, rpm	1800
Compression ratio	7.0
Oil temperature, °F	150
Coolant temperature, °F	250
Inlet-air temperature, °F	150, 200, 250
Spark advance, degrees B.T.C.	20, 30

The fuel used was AN-F-28, Amendment-2.

Pressure cards were obtained with a Farnboro pressure indicator with a thyratron circuit to provide the spark voltage. (See references 7 and 8.) The balanced-pressure-disk pickup used with this instrument was placed in hole B (fig. 5) when pressure cards were being taken. The average crank angle at which knock occurred was recorded on these indicator cards with the aid of a contactor and the thyratron circuit. This contactor was set by observing the position on the oscilloscope screen of the impulse trace induced by the sparking of the thyratron circuit relative to the sudden amplitude increase of the vibration trace at the time of knock. Pressure data and the average crank angle of knock occurrence were obtained as a function of fuel-air ratio on the same day and under the same engine conditions as each of the frequency-data tests.

During tests run with a shrouded valve, the variation with fuel-air ratio of the mean cylinder gas temperature was determined by placing a platinum to platinum-rhodium thermal plug (deactivated with TEL) in hole A or B (fig. 5). The thermal-plug leads were connected to a Brown self-balancing potentiometer and readings were taken at each of the data points at which gas-vibration traces were photographed.

A magnetostriction pickup was placed in hole A or B (fig. 5) to obtain gas-vibration traces on an oscilloscope screen. In preliminary tests a piezoelectric quartz pickup and a diaphragm induction-type pickup were used to check the frequencies obtained with the magnetostriction pickup.

In order to facilitate the study of the gas vibrations, the magnetostriction pickup leads were passed to a 4,000 to 10,000 cycles per second band-pass filter and thence to the oscilloscope. The engine-cycle pressure trace was thus eliminated and only the pressure fluctuations due to gas vibrations having frequencies in the pass band were visible on the oscilloscope screen.

A 35-millimeter camera having an f/1.9 maximum aperture was used to photograph the vibration traces appearing on the oscilloscope screen. The shutter speed was so adjusted that the shutter would be open for a period of time slightly greater than that of one complete engine cycle. The horizontal sweep of the oscilloscope was synchronized with the engine cycles by means of a contactor operated by gearing it to the crankshaft at a ratio of 2:1.

The reference time scale was provided by a calibrated commercial oscillator, whose output was applied to the oscilloscope and recorded along with each gas-vibration trace. The reference trace and the gas-vibration trace were photographed on each frame by double exposure. The reference frequency was set at 5000 cycles per second during all tests.

Because, at a constant fuel-air ratio, considerable cycle-to-cycle variation was found to occur in the frequency of knock-induced cylinder gas vibrations, it was necessary to take the average of several traces as the frequency to be ascribed to a particular fuel-air ratio. In each test between 12 and 16 traces were therefore photographed at each of 10 fuel-air ratios. All data were taken at barely audible knock intensity. The frequencies of the photographed vibration traces and the reference frequency traces were measured with a projector having a graduated distance scale. In all photographs showing definite knock, the five cycles following the occurrence of knock were measured and compared with five cycles of the reference trace. In some photographs no definite evidence of the occurrence of knock appeared, but mild gas vibrations were visible; in these cases the five cycles beginning at the normal crank angle of knock occurrence were measured. This crank angle was determined from the position at which knock occurred in other photographed traces.

PRESENTATION OF RESULTS

<u>Types of vibration trace.</u> - Although all vibration-trace photographs were taken under knocking conditions, a considerable variety of traces was observed. This variety was evident in each of the

series of about 15 traces photographed at a fixed fuel-air ratio. The traces obtained were arbitrarily divided into six types of which five are represented in photographs reproduced in figure 6. In these photographs, the A indicates the crank angle at which knock normally occurred. The frequencies are the mean of the five vibration cycles immediately following A. The percentage distribution of the types varied considerably with fuel-air ratio and depended even more upon whether a shrouded or an unshrouded intake valve was used. Traces were classified according to the following descriptions:

Type I (figs. 6(a), (b), and (c)): Definite knock preceded by vibrations of medium amplitude relative to that of the knock-induced vibrations. The type is characterized by the occurrence of about 5 to 10 cycles of preknock vibrations followed by the sharp increase and gradual decrease in vibration amplitude associated with the occurrence of knock. The character of the preknock vibrations varied and may be classified as follows: (a) amplitude increasing gradually until knock occurs; (b) amplitude increasing more rapidly and maintaining an approximately constant value until knock occurs; and (c) amplitude increasing rapidly and decreasing slightly before knock occurs. These subtypes may be seen, respectively, in figures 6(a), (b), and (c). With an unshrouded valve installed, preknock vibrations of subtype (c) decreased in amplitude much more sharply than appears in figure 6(c) and were more frequent than in tests in which a shrouded valve was used. The reality of preknock vibrations has been definitely established by analyses of high-speed motion pictures of knocking cycles. (See reference 9.)

Type II (figs. 6(d), (e), and (f)): Definite knock preceded by vibrations of amplitude approaching that of the knock-induced vibrations. The three subtypes of preknock vibration described in the preceding paragraph were also observed in this category; subtypes (b) and (c) were the most common. Figure 6(e) is especially interesting in that the normal knock-induced vibrations seem to be superimposed upon the high-amplitude preknock vibrations of subtype (b). Few traces of this peculiar character were encountered.

Type III (figs. 6(g) and (h)): Definite knock preceded by vibrations having a small amplitude relative to that of knock-induced vibrations. With the shrouded valve, this type was predominant in the lean-mixture region. The amplitude of the preknock vibrations appearing in this category is comparable with the amplitude of vibrations encountered with inlet-air pressure several inches of mercury below the knock limit.

Type IV (figs. 6(i), (j), and (k)): Gradual increase and decrease in vibration amplitude with no definite evidence of the occurrence of knock. This type of trace was predominant in the rich-mixture region when the shrouded valve was used. About one-fourth of the traces in this category showed evidence of what seems to be destructive interference similar to that encountered consistently in type V. (Cf. figs. 6(j) and (l).) When this interference was present it was impossible to determine the frequency of the first five cycles following the normal crank angle of knock occurrence because the distance between peaks was disturbed. This subtype, therefore, is not included in the determination of mean vibration frequencies. All other traces in this category, however, are included. The crank angle of maximum vibration amplitude, in most traces of this type, corresponded within one vibration cycle with the normal crank angle of knock occurrence, which seems to indicate that knock actually occurred in most of these cycles but was of insufficient intensity to induce gas vibrations having amplitude greater than the preknock vibrations.

Type V (fig. 6(l)): Preknock vibrations followed by an abrupt decrease in vibration amplitude at the normal crank angle of knock occurrence. The destructive interference evident in this type is perhaps due to the occurrence of knock-induced vibrations whose displacement is out of phase with that of preknock vibrations. This category was not included in determinations of mean frequencies.

Type VI (not shown): Vibrations of amplitude too small for measurement throughout the preknock and knock period. This type was not included in determinations of mean vibration frequencies.

Table III is a summary of the type distribution of the photographed vibration traces for three fuel-air-ratio ranges and for tests with the shrouded and with the unshrouded valve. In the determination of mean vibration frequencies, all traces of types I, II, and III were used and all traces of type IV except those showing destructive interference. Types V and VI were not included.

The relative distribution of the types showing definite knock or large-amplitude gas vibrations is seen to be dependent upon the fuel-air ratio, as well as upon the type of valve used. (The use of the shrouded valve is known to increase the turbulence of the charge and likewise the reproducibility of knocking cycles.) It may be concluded that analyses of single knocking cycles, or analyses of knocking combustion based on one set of engine conditions, should not be expected to give results which are true for all knocking cycles or any engine conditions. It is seen that the relative amplitude of preknock vibrations is variable, even under constant engine conditions, and is quite independent of knock intensity. These experiments also indicate that gas vibrations may occur independently of the occurrence of knock.

Reliability of the frequency measurement. - The large amplitude of the preknock vibrations appearing in many of the recorded traces was somewhat unexpected and might be thought to represent spurious vibrations due to inadequacies in the mechanical or electrical systems. An investigation of the transient characteristics of the pickup and filter combination, however, did not support this assumption. Traces obtained by mechanically tapping the pickup showed sharp exponential decrease in amplitude of vibration. In four cycles the amplitude was reduced to one-fourth that of the maximum cycle. Because all photographed gas-vibration traces showed a much more gradual decrease, transient vibrations, if any were excited by knock, were not dominant over gas-pressure oscillations. It seems possible, however, that vibrations having frequencies near the natural frequency of the pickup would be accentuated beyond their true relative amplitude because of resonance. This effect is apparently negligible, since the traces in the medium-mixture range, where frequencies are not near the natural frequency (about 6380 cps), had about the same distribution in types of trace as did the rich-mixture region, where frequencies are near the natural frequency. The lean-mixture traces showed more heavy-knock traces, but this tendency is recognized as characteristic of the mixture range and not of the pickup.

Other evidence that the frequency and the relative amplitude of the preknock and the knock-induced cylinder gas vibrations are largely independent of pickup characteristics is provided by the results obtained using a piezoelectric quartz pickup and a diaphragm induction-type pickup. Both of these pickups recorded vibrations whose frequencies were distributed over the same range as those obtained with the magnetostriction pickup. The types of trace obtained were also similar, except that those obtained with the quartz pickup showed very little evidence of interference.

The initial shock wave associated with knock is not recorded on the photographed traces. When a band-pass filter is used, a time delay is to be expected for pulses having too sharp a time-of-rise. This effect was plainly visible in all photographs showing definite knock and in the traces produced by mechanically tapping the pickup. The first cycle showing an abrupt increase in amplitude was always lower than the second. The second, however, invariably had the greatest amplitude, indicating that the time delay introduced by the filter circuit influenced the relative amplitude of only the first cycle.

Much of the frequency data reported herein was obtained with the pickup located in the slanted top cylinder hole; the rest was obtained with the pickup in the hole opposite the spark plugs. The mean frequencies were found to be the same in either case within the normal range of variation. That these frequencies should be independent of the location of the pickup in the cylinder is to be expected from the consideration that the gas vibrations include the entire combustion space and should therefore at any instant have a frequency determined by the average condition of the entire charge.

In a preliminary test it was determined that the intensity of knock had no noticeable effect upon the mean gas-vibration frequency. Variations in inlet-air pressure up to 3 inches of mercury above the barely audible knock limit resulted in vibration frequencies whose variation at constant fuel-air ratio was over the same range as that at barely audible knock. The occurrence of knock was also found to increase the amplitude of the vibrations without altering their frequencies beyond the extremes encountered at a given fuel-air ratio. Traces showing no definite evidence of knock occurrence had frequencies over the same range as those showing definite knock. This fact indicates that the intensity of knock did not affect the average gas temperature appreciably. The destructive effects of knock may therefore be due to detonation forces, chemically active products of combustion, or to increases in heat-transfer rates rather than to large increases in the average gas temperature in the cylinder.

Frequency data. - Figure 7 is a plot of the frequencies of all measured vibration traces in a single typical test run. A partial explanation of the observed frequency distribution at a fixed fuel-air ratio is probably to be found in the cycle-to-cycle variation in fuel-air ratio, turbulence, fuel mixing, and ignition lag. A measuring uncertainty of about 100 cycles per second, due to the width of the oscilloscope trace, further accounts for the spread. (A similar cyclic variation is evident in flame temperatures measured in a Diesel engine by means of the newly developed electro-optical pyrometer, described in a paper "Flame-Temperature Measurements in Internal-Combustion Engines" presented before the A.S.M.E. at a Cleveland, Ohio meeting in May 1945.)

The mean frequencies and the temperatures recorded by the platinum to platinum-rhodium thermal plug are plotted against fuel-air ratio for tests run at inlet-air temperatures of 150°, 200°, and 250° F in figure 8. It is seen that, although the scatter in mean-frequency points is considerable, there is a definite and quite consistent variation with fuel-air ratio. The shrouded-valve curves for inlet temperatures of 150° and 200° F average two test runs; the shrouded-valve curve for inlet temperature of 250° F averages three.

Figure 8 also includes a plot of the mean frequencies and the thermal-plug temperatures for the test in which the charge was fired on alternate cycles and a plot of the mean frequencies for the tests run with an unshrouded valve. Of the unshrouded-valve tests, two were run with a spark advance of 20° B.T.C., as were all shrouded-valve tests, and one was run with a spark advance of 30° B.T.C.

Pressure data. - Figure 9 presents peak pressures, air flows, and indicated mean effective pressures for each of the test conditions for which frequency data were obtained. These data were obtained on the same day as the frequency data for the corresponding engine conditions.

Peak temperatures calculated from the peak-pressure curves of figure 9 are plotted in figure 10 for inlet-air temperatures of 150°, 200°, and 250° F. Figure 10 also includes the peak temperatures calculated for the test in which the charge was fired on alternate engine cycles and for the tests run with an unshrouded valve. These temperatures were calculated from the simple gas-law equation:

$$T = PV/NR \tag{5}$$

where

T peak temperature, °R

P peak pressure, pounds per square foot

V volume of combustion chamber at average crank angle of peak pressure, cubic feet

N number of moles of charge in the cylinder

R gas constant, 1546 foot-pounds per mole per °R

The molecular weights required to calculate N were obtained from the calculations of percentage composition of the products of combustion. (See appendix B.) The curves of figure 10 are uncorrected for the presence of residuals or for gas imperfections. For shrouded-valve tests, V is the combustion-space volume at a crank angle of 10° A.T.C., which was the average crank angle of peak pressure. (See fig. 12.) Similarly, for the unshrouded-valve tests, the combustion-space volume at 14° A.T.C. was assumed for a spark advance of 30° B.T.C. and that at 20° A.T.C. for a spark advance of 20° B.T.C.

Figure 11 shows the relation between temperatures calculated from peak pressures and from pressures existing 5° after the peak and the extent to which the corrections for residuals and for gas imperfections affect these temperatures. The corrections were applied to the peak-temperature curve obtained with a shrouded valve at an inlet-air temperature of 200° F. The corrected pressure-derived peak temperatures for tests in which a shrouded valve was used are in good agreement with those obtained from thermodynamic charts and temperatures 5° after the peak are about 200° F lower than peak temperatures at the fuel-air ratio of maximum temperature. (Temperatures 5° after the peak were calculated because they are more nearly comparable with frequency-derived temperatures, as explained in the discussion of fig. 13.)

The crank angles of the arrival of the flame front at the rear cylinder wall, of peak pressure, and of the average occurrence of knock are plotted as functions of fuel-air ratio in figure 12. The methods of obtaining the crank angles of average knock occurrence and peak pressure have already been described. The crank angle at which the flame front arrived at the rear cylinder wall was determined by placing an ionization gap in the cylinder hole opposite the spark plugs. The curves show that peak pressure, knock, and the completion of burning all occurred at a considerably later crank angle when an unshrouded valve was used. It is also seen that, although the average crank angle of knock occurrence was, within experimental error, the same as the crank angle of peak pressure when a shrouded valve was used, knock occurred on the average several degrees after peak pressure when an unshrouded valve was installed. With the shrouded valve, the flame front had traversed the combustion chamber about 8° crank angle (or about 750 microsec) before average knock occurred, except in the very rich-mixture region. This phenomenon was also mentioned in reference 9. With the unshrouded valve the cyclic variation in the time of flame-front arrival was too great to permit making a similar comparison.

Comparison of temperatures. - Figure 13 is a comparison plot of (1) temperatures obtained from the frequency curves of figure 8; (2) pressure-derived peak-temperature curves of figure 10; (3) peak temperatures obtained from the thermodynamic charts of references 6 and 10; and (4) the thermal-plug temperatures of figure 8. The cylinder gas-vibration frequencies were converted to temperatures by using the chart shown in figure 4. These temperatures should be the mean temperatures of the cylinder gases over the portion of the engine cycle represented by the five gas-vibration cycles following the normal crank angle of knock occurrence. For the test run with a shrouded valve the normal crank angle of knock occurrence was, within an error of 2° crank angle, the same as the crank angle of peak pressure. Inasmuch as the five measured gas-vibration cycles occupy about 5/6000 second, or about 9° crank angle at an engine speed of 1800 rpm, the average cylinder gas pressure and volume during these cycles are those existing about 5° crank angle after the attainment of peak pressure. Temperatures calculated from the pressures and volumes existing at this crank angle were from 0 to 4 percent lower than peak temperatures; the extent of the decrease was greatest at the fuel-air ratio of maximum temperature and less at richer and leaner mixtures. Correction of the pressure-derived temperatures for the presence of residuals and for high-pressure gas imperfections results in further decreases. These corrections were calculated for one temperature curve by the methods outlined in appendix C. The correction factors for gas imperfections are summarized in table IV. The effects of these corrections on peak temperatures are shown in figure 11.

DISCUSSION

The validity of the assumptions used to calculate cylinder gas temperatures from cylinder gas-vibration frequencies may be judged from the following considerations: From figure 13 it is seen that the only engine condition for which temperatures calculated from frequency data and from pressure data are in fairly close agreement is the one in which an unshrouded valve was used with a spark advance of 30° B.T.C. The frequency-derived temperatures did not increase when a shrouded valve was used, nor did they decrease when the spark was retarded to 20° B.T.C. with an unshrouded valve. The only difference noted between frequencies obtained with the shrouded valve and those obtained with an unshrouded valve was a shift in the fuel-air ratio at which maximum temperature occurred. This shift was quite consistent throughout the combustible fuel-air-ratio range in that the curve obtained with an unshrouded valve at a spark advance of 20° B.T.C. would coincide with that obtained with a shrouded valve under the same engine conditions if translated about 0.006 fuel-air-ratio units. No such fuel-air-ratio shift appears in temperatures calculated from pressure data, which indicates that the explanation lies in some effect of the shrouded valve upon sound velocity in the combustion chamber. The fact that frequencies stayed at about the same values for the unshrouded as for the shrouded valve, whereas temperatures calculated from pressure data changed greatly, indicates either that the dependence of cylinder gas-vibration frequencies upon temperature is not so simple as was assumed or that the pressure data are not dependable. Further investigation will be required before the factors affecting the frequency of these vibrations can be determined.

It is interesting to note, however, that frequency-derived temperatures exhibit a variation with inlet-air temperatures similar to that of the mean thermal-plug temperatures. (See fig. 13.) The decrease of these temperatures with increased inlet-air temperature is to be expected from the consideration that the heat transfer to the cylinder walls per unit charge weight decreases as the charge weight is increased. (See reference 11.) The fact that this effect is noticeable in the frequency-derived temperature curves indicates that, under certain conditions, this method of determining cylinder gas temperatures is quite sensitive. Temperatures calculated from peak-pressure data do not reveal this effect. The spread between the pressure-derived temperature curves with the shrouded valve at different inlet-air temperatures is considerably greater near the fuel-air ratio of maximum temperature than that shown by curves from the thermodynamic charts or by frequency-derived temperature curves. This spread must be attributed to the greater experimental error present in pressure-derived temperatures due to errors in the pressure-indicating apparatus and to uncertainties in the charge weight.

Another indication that under certain conditions frequency-derived temperatures behave according to the expectations of simple sound theory is given by the fact that higher frequencies were obtained when the charge was fired on alternate engine cycles. An increase in cylinder gas temperatures under these conditions is to be expected because of the absence of exhaust-gas dilution. This increase is also evident in the pressure-derived temperature curves. The alternate-cycle firing test was run to determine whether the presence of residuals may have caused the difference in fuel-air ratio between the peaks of the frequency-derived temperature curves, and those of the curves obtained from pressure data and thermodynamic charts. Figure 13 shows that the elimination of residuals had no noticeable effect on the variation of the frequency-derived temperatures with fuel-air ratio.

The data obtained in this investigation cannot as yet be considered conclusive. Two phenomena revealed by these data remain unexplained: the shift in fuel-air ratio of the frequency-derived temperature curves when a shrouded valve is replaced with an unshrouded one and the fact that frequency-derived temperatures remained about the same in value under engine conditions for which pressure-derived temperatures varied widely.

With regard to the disagreement between pressure-derived and frequency-derived temperatures, reference may be made to the data obtained by Hershey and Paton (reference 12) by the sodium line-reversal method. The experimental temperatures that they obtained were, like the frequency-derived temperatures of the present investigation, from 600° to 1000° F lower than the theoretical temperatures over the entire fuel-air-ratio range. Their data further indicated that the effect of spark advance on peak temperatures was very small, which is in agreement with the frequency-derived temperature data reported herein. These agreements argue well for the validity of the method of determining gas temperatures from gas-vibration frequencies and throw doubt upon the accuracy of temperatures obtained from pressure data. Further determinations of temperature by the line-reversal method may be found in references 13 and 14, but these reports are not useful for comparison because the engine conditions that were varied were not the same as those varied in this investigation. The temperatures, however, are, where comparison is possible, in approximate agreement with the frequency-derived temperatures presented in this report.

SUMMARY OF RESULTS

The results of this investigation to determine the temperature of cylinder gases from the frequency of knock-induced cylinder gas vibrations may be summarized as follows:

1. Temperatures calculated from frequency data were in agreement with temperatures measured by the spectral line-reversal method in previous investigations and were about 700° F lower than temperatures obtained from thermodynamic charts. Temperatures obtained from peak-pressure data were found to be in poor agreement with frequency-derived temperatures.

2. A maximum error of only about 3.5 percent would be introduced in temperatures calculated from frequency data if the variation of the ratio of specific heats with fuel-air ratio and temperature were neglected.

3. A maximum error of about 14 percent would be introduced in frequency-derived temperatures if the variation of molecular weight with fuel-air ratio were neglected. The variation of molecular weight with temperature, however, is less than 2 percent between 2500° and 5000° F.

Aircraft Engine Research Laboratory,
National Advisory Committee for Aeronautics,
Cleveland, Ohio.

APPENDIX A

CORRECTION OF THE SOUND-VELOCITY EQUATION FOR GAS IMPERFECTIONS

In the derivation of equation (4) for the relation between frequency and temperature, the ideal-gas equation of state was assumed. In order to correct for the characteristics of real gases, the sound-velocity equation should be written in the differential form

$$c^2 = -\frac{V^2}{M}\left(\frac{dP}{dV}\right)_{ad} \tag{6}$$

where V and M are the molar volume and the molecular weight, respectively, and $(dP/dV)_{ad}$ indicates adiabatic differentiation of a correct equation of state. Using the Beattie-Bridgeman equation and neglecting correction terms beyond the first order

$$P = RT/V + RTB_o/V^2 - A_o/V^2 \tag{7}$$

where A_o and B_o are constants depending only on the composition of the gas. Differentiation with respect to V yields:

$$dP/dV = (R/V + RB_o/V^2)dT/dV - RT/V^2 - (RTB_o - A_o)2/V^3 \tag{8}$$

For an adiabatic process

$$c_v dT = -PdV \tag{9}$$

where c_v is the specific heat at constant volume. When equation (7) is substituted in (9)

$$dT/dV = -RT/c_v(1/V + B_o/V^2) + A_o/V^2c_v \tag{10}$$

If equations (8) and (10) are combined, the terms rearranged, and since $R/c_v \approx \gamma - 1$, the velocity of sound in real gases is

$$c^2 = \frac{\gamma RT}{M}\left[1 + 1/V\left(2B_o - \frac{A_o(\gamma + 1)}{\gamma RT}\right) + \frac{B_o(\gamma - 1)}{\gamma RTV^2}(B_oRT - A_o)\right] \tag{11}$$

The last term in the brackets is found to be negligibly small. Table V gives the correction term $1/V\left[2B_o - A_o(\gamma + 1)/\gamma RT\right]$ at four fuel-air ratios for a typical test run using a shrouded valve and an inlet-air temperature of 200° F, with an assumed γ of 1.26.

The values of B_o and A_o for the products of combustion were obtained by the same method as that used for obtaining b' in appendix C; the constants for each constituent were obtained from reference 15. It is seen from table V and equation (11) that the correction for gas-law imperfections would lower the frequency-derived temperature curves of figure 13 about 1.5 percent near the peaks and about 3 percent at the richest fuel-air mixture. At the present stage of development of the process of obtaining temperatures from gas-vibration frequencies, this correction is considered to be of little significance and has not been applied in the frequency-temperature computations.

APPENDIX B

CALCULATION OF THE COMPOSITION AND THE RATIO OF SPECIFIC HEATS OF THE PRODUCTS OF COMBUSTION OF FUEL-AIR MIXTURES AT HIGH TEMPERATURES

In order to determine accurately the values of γ and M to be used in calculating temperatures from frequency data, accurate data had to be obtained on the composition of the cylinder charge over the entire combustible fuel-air-ratio range at the temperatures attained during combustion. Because dissociation and recombination equilibrium reactions take place to a noticeable extent at these temperatures, it was recognized that composition data obtained from exhaust-gas analyses might not be valid for use in computing the γ and M of the charge. Some high-temperature composition data were calculated in 1936 by Hershey, Eberhardt, and Hottel (reference 6, appendix B), but the assumed fuel composition $(CH_{2.25})_x$ was different from that used in this investigation, and the fuel-air ratios for which compositions were computed covered too small a range to be of value. The method of reference 6, however, which is based upon known equilibrium reactions and dissociation constants, was used to compute the composition of the products of combustion with dry air of $(CH_2)_x$ fuel (H/C = 0.168), which is similar to that used in this investigation, over a large temperature and fuel-air-ratio range. The equations used, derived in reference 6, are as follows:

$$H_2O = \frac{4H_2\left[N_2 - 3.76AH_2 - 1.88AK_1(H_2)^{1/2}\right]}{15.04AH_2 + 7.52AK_4(H_2)^{1/2} - 2K_7(N_2)^{1/2}}$$

$$NO = K_7 \frac{H_2O(N_2)^{1/2}}{H_2}$$

$$CO = \frac{K_5H_2(N_2 + NO/2)}{3.76A(H_2O + K_5H_2)}$$

$$CO_2 = (CO)(H_2O)/K_5H_2$$

$$OH = K_4H_2O/(H_2)^{1/2}$$

$$O_2 = K_3(H_2O/H_2)^2$$

$$H = K_1(H_2)^{1/2}$$

$$O = K_2(O_2)^{1/2}$$

In these equations, the chemical symbols represent volume fractions and the K's are dissociation constants that may be found as functions of temperature in reference 6, appendix B. The constant A depends on the total number of moles of O_2 per carbon atom at the fuel-air ratio and for the particular fuel for which calculations are being made. For $(CH_2)_x$ fuel,

$$A = \frac{1.5(F/A)_{stoic}}{F/A} = 1.5 \times 0.068/(F/A)$$

where F/A is the fuel-air ratio and the subscript stoic indicates the stoichiometric mixture. Computations were made for seven fuel-air ratios and for several temperatures in the range from 2500° to 5000° F.

Table I summarizes the results of these calculations. In figure 1 the calculated compositions are compared with those obtained from the exhaust-gas analyses of reference 16. It is seen that the two methods give very similar results and that the differences are those to be expected from a consideration of the dissociation equilibria existing at the higher temperatures.

If the percentage composition of the charge and the specific heats of the constituents as a function of temperature are known, it is possible to calculate a weighted mean specific heat, which should be the specific heat of the mixture of gases comprising the products of combustion. Such calculations were made over the entire fuel-air-ratio and temperature range of interest in this investigation. The specific heats of the constituents have been determined very accurately from spectroscopic data. A tabulation of the specific heats of O_2, N_2, CO_2, CO, H_2, and H_2O from 600° to 5400° R may be found in references 17 and 18. The data on H_2O are faulty in reference 17 and should be obtained from the corrected table in reference 18. The specific heats of NO and OH were obtained from the original computations in references 19 and 20, respectively. Figure 3 is a plot of the specific-heat data used in the present computations. The variation with pressure of these data is negligible, in the indicated temperature range, for pressures attained in an engine cylinder. (See reference 15.)

The following equation was used to compute the specific heats of the products of combustion at fuel-air ratio F/A and temperature T:

$$\bar{c}_p = \Sigma\, v c_p$$

where

$\bar{c}_p$ specific heat of the combustion products at F/A and T, Btu/(mole)(°R)

v volume fraction of the individual constituent at F/A and T

c_p specific heat of the individual constituent at T, Btu/(mole)(°R)

The summations were made over the eight constituents shown in figure 3. The products O and H were not included, inasmuch as their contribution was found to be negligibly small over the entire fuel-air-ratio range. (See table I.) From these weighted mean specific heats, the weighted mean ratio of specific heats of the mixture at F/A and T was computed from the formula:

$$\gamma = \bar{c}_p \Big/ (\bar{c}_p - R)$$

where R equals 1.986 Btu/(lb-mole)(°R)

In order to be consistent in carrying out these calculations, it would be necessary to calculate the percentage composition at each of the temperatures for which the weighted specific heats were calculated. It is evident from figure 2, however, that the variation of composition with temperature is very small relative to its variation with fuel-air ratio. If, therefore, a composition is assumed for a temperature somewhere in the range for which γ is computed, no appreciable error will result if the variation of composition with temperature is neglected.

Figure 4 is a plot of the calculated values of γ against temperature for several fuel-air ratios. The constant-frequency lines were superimposed upon this plot by the use of equation (4). The compositions assumed in calculating γ are indicated by the footnote in table I. The molecular weights used and the resulting values of γ are summarized in table II.

Dr. Glenn C. Williams of Massachusetts Institute of Technology has noted that, if γ defined as the ratio of the specific heats of the gases at equilibrium is replaced by an "effective" γ defined as $(\partial H/\partial T)_P / (\partial E/\partial T)_V$ - where H is enthalpy and E is internal energy - and calculated from thermodynamic charts (see reference 10), the resulting cylinder gas temperatures measured from vibration frequencies would be 4 to 7 percent higher than those reported. The difference between the two methods lies in the inclusion of the point-to-point association and dissociation energy on the thermodynamic charts. The actual temperature probably lies between the extremes of the two methods.

APPENDIX C

CORRECTION FACTORS FOR TEMPERATURES CALCULATED FROM THE SIMPLE GAS-LAW FORMULA $T = PV/NR$

The use of a modified van der Waals equation of state permits the calculation of the discrepancies from the ideal-gas law due to high pressure. This equation may be written as follows (see reference 21, p. 2):

$$PV/RT = 1 + \frac{b - a/RT}{V} + 0.625\ b^2/V^2 + 0.2869\ b^3/V^3 + 0.1928\ b^4/V^4$$

Reference 21 presents (p. 51) a table of the van der Waals b's for all molecules comprising the products of combustion at a temperature of 6480° R and indicates that the assumption that these are independent of temperature in the range between 2700° and 9000° R is justified. On the same page is a table giving values of PV/RT as a function of $b'\rho$ where b' is the van der Waals constant of the gas mixture being considered and ρ is its density. The van der Waals a was, as in reference 21, considered to be negligible in the temperature range of interest in this investigation.

The b' for the products of combustion of a fuel-air mixture is the mean b, based on partial pressure, of the constituents:

$$b' = \frac{\Sigma(vb)}{M}$$

where

b coefficient of individual constituent, $cm^3/mole$

v volume fraction of individual constituent

M mean molecular weight of mixture

b' resulting coefficient of mixture, $cm^3/gram$

The charge density was calculated from air-flow and fuel-flow data at several fuel-air ratios for a shrouded valve test at an inlet-air temperature of 200° F. The values of the density correction factor PV/RT calculated for these conditions are summarized in table IV.

The correction for the presence of residuals was obtained by assuming the percentage of residuals to be that given by the thermodynamic charts of references 6 and 10 for the conditions of a particular test run. The charts gave a percentage of residuals varying from about 4 percent in the lean-mixture region to about 2.2 percent at a fuel-air ratio of 0.085. An average value of 3 percent was assumed for all fuel-air ratios, making the correction factor for the presence of residuals simply 1/1.03, or 0.97.

In order to obtain the temperature of the cylinder gases 5° crank angle after the attainment of peak pressure from the temperature at peak pressure, the peak temperature must be multiplied by the ratio of the product of pressure and volume 5° after the peak to the same product at peak pressure.

These considerations result in the following equation for obtaining corrected temperatures 5° after peak from uncorrected peak temperatures:

$$T_2 = 0.97\ (RT/PV)(P_2V_2/P_1V_1)\ T_1$$

where

T_1 uncorrected peak temperature

RT/PV reciprocal of the density correction factor

P_2V_2 pressure and volume 5° crank angle after the attainment of peak pressure

P_1V_1 peak pressure and volume

T_2 corrected temperature 5° crank angle after attainment of peak pressure

For a shrouded-valve test run, with an inlet-air temperature of 200° F, the effect of the various correction factors upon uncorrected peak temperatures is illustrated in the plot of figure 11.

REFERENCES

1. Kudryavtsev, B. B.: The Velocity of Sound in Reacting Mixtures. Chem. Abs., vol. 37, no. 22, Nov. 20, 1943, p. 6526. (Abs. from Trudy Moskov., Khim.-Tekh. Inst. im. Mendeleeva 1940, no. 7, pp. 142-145; Khim. Referat. Zhur., vol. 4, no. 7-8, 1941.)

2. Kantrowitz, Arthur: Effects of Heat Capacity Lag in Gas Dynamics. NACA ARR No. 4A22, 1944.

3. Wawrziniok: Pressure Rise, Gas Vibrations, and Combustion Noises during the Explosion of Fuels. NACA TM No. 711, 1933.

4. Draper, C. S.: The Physical Effects of Detonation in a Closed Cylindrical Chamber. NACA Rep. No. 493, 1934.

5. Miller, Cearcy D., and Olsen, Lowell H.: Identification of Knock in NACA High-Speed Photographs of Combustion in a Spark-Ignition Engine. NACA ARR, Feb. 1943.

6. Hershey, R. L., Eberhardt, J. E., and Hottel, H. C.: Thermodynamic Properties of the Working Fluid in Internal-Combustion Engines. SAE Jour. (Trans.), vol. 39, no. 4, Oct. 1936, pp. 409-424.

7. Collins, John H., Jr.: Alterations and Tests of the "Farnboro" Engine Indicator. NACA TN No. 348, 1930.

8. Taylor, E. S., and Draper, C. S.: A New High-Speed Engine Indicator. Mech. Eng., vol. 55, no. 3, March 1933, pp. 169-171.

9. Miller, Cearcy D., and Logan, Walter O., Jr.: Preknock Vibrations in a Spark-Ignition Engine Cylinder as Revealed by High-Speed Photography. NACA ARR No. E4J25, 1944.

10. McCann, W. J.: Thermodynamic Charts for Internal-Combustion-Engine Fluids. NACA RB No. 3G28, 1943.

11. Pinkel, Benjamin, and Ellerbrock, Herman H., Jr.: Correlation of Cooling Data from an Air-Cooled Cylinder and Several Multicylinder Engines. NACA Rep. No. 683, 1940.

12. Hershey, Albert E., and Paton, Robert F.: Flame Temperatures in an Internal Combustion Engine Measured by Spectral Line Reversal. Eng. Exp. Sta. Bull. No. 262, Univ. Ill., Oct. 1933.

13. Rassweiler, Gerald M., and Withrow, Lloyd: Flame Temperatures Vary with Knock and Combustion-Chamber Position. SAE Jour., vol. 36, no. 4, April 1935, pp. 125-133; discussion, pp. 133-136.

14. Brevoort, Maurice J.: Combustion-Engine Temperatures by the Sodium-Line Reversal Method. NACA TN No. 559, 1936.

15. Ellenwood, Frank O., Kulik, Nicholas, and Gay, Norman R.: The Specific Heats of Certain Gases over Wide Ranges of Pressures and Temperatures, Air, CO, CO_2, CH_4, C_2H_4, H_2, N_2, and O_2. Eng. Exp. Sta. Bull. No. 30, Cornell Univ., Oct. 1942.

16. Gerrish, Harold C., and Voss, Fred: Interrelation of Exhaust-Gas Constituents. NACA Rep. No. 616, 1937.

17. Heck, Robert C. H.: The New Specific Heats. Mech. Eng., vol. 62, no. 1, Jan. 1940, pp. 9-12.

18. Heck, Robert C. H.: The New Specific Heats - Addenda. Mech. Eng., vol. 63, no. 2, Feb. 1941, pp. 126-138; discussion, pp. 128-135.

19. Johnston, Herrick L., and Chapman, Alan T.: Heat Capacity Curves of the Simpler Gases. I. Heat Capacity, Entropy and Free Energy of Gaseous Nitric Oxide from Near Zero Absolute to 5000° K. Jour. Am. Chem. Soc., vol. 55, no. 1, Jan. 1933, pp. 153-172.

20. Johnston, Herrick L., and Dawson, David H.: Heat Capacity Curves of the Simpler Gases. III. Heat Capacity, Entropy and Free Energy of Neutral OH from Near Zero Absolute to 5000° K. Jour. Am. Chem. Soc., vol. 55, no. 7, July 1933, pp. 2744-2753.

21. Hirschfelder, J. O., McClure, F. T., Curtiss, C. F., and Osborne, D. W.: Thermodynamic Properties of Propellent Gases. NDRC Rep. No. A-116, Nat. Defense Res. Committee, Nov. 23, 1942. (Extension and Revision of NDRC Rep. No. A-48 (OSRD No. 547).)

TABLE I

CALCULATED COMPOSITION OF THE PRODUCTS OF COMBUSTION WITH DRY AIR OF A FUEL HAVING THE FORMULA $(CH_2)_x$

[Hydrogen-carbon ratio = 0.168]

Fuel-air ratio	Temperature (°K)	Percentage by volume									
		N_2	H_2	H_2O	CO_2	O_2	CO	NO	OH	H	O
0.050	1800	75.0	1.85×10^{-4}	9.73	9.75	5.54	0	0	0	0	0
	2200[a]	74.65	.0053	9.66	9.69	5.03	.03	.63	.24	0	0
	2600	74.2	.0435	9.21	9.41	4.50	.28	1.29	.81	0	.05
	3000	73.5	.20	8.47	8.30	4.32	1.35	2.17	1.89	.07	.24
0.06	2400[a]	74.1	0.04	11.50	11.32	1.76	0.31	0.42	0.42	0	0
0.07	1800	73.3	0.25	13.09	12.45	0	0.90	0	0	0	0
	2600[a]	72.6	.30	12.75	11.58	.18	1.69	.26	.42	.02	.01
	3000	71.4	.64	11.66	9.50	.79	3.61	.94	1.46	.13	.11
0.08	2600[a]	70.35	1.25	13.27	9.10	0	5.52	.11	.32	0	0
	3000	69.7	1.40	12.52	8.17	.19	6.33	.45	1.06	.19	.05
0.09	1800	68.2	3.40	12.50	7.84	0	8.08	0	0	0	0
	2600[a]	68.1	2.70	13.09	6.96	0	8.93	.03	.14	.07	0
	3000	67.6	2.60	12.67	6.51	.06	9.26	.24	.78	.26	.03
0.10	2400[a]	65.9	4.55	12.40	5.30	0	11.85	0	0.09	0	0
	2800	65.6	4.40	12.40	5.10	0	11.93	.05	.26	.18	0
0.115	1800	62.6	8.50	10.20	4.49	0	14.23	0	0	0	0
	2200[a]	62.6	7.90	10.70	3.90	0	14.80	0	.02	0	0
	2400	62.6	7.80	10.87	3.64	0	15.08	0	.03	.05	0
	2800	62.4	7.60	10.75	3.30	0	15.40	.04	.30	.27	0
	3000	62.3	7.60	10.63	3.14	0	15.55	.07	.39	.45	.01

[a]The compositions for these temperatures are the ones used in computing the ratios of specific heats of the combustion products.

National Advisory Committee
for Aeronautics

TABLE II

CALCULATED MEAN MOLECULAR WEIGHT AND RATIO OF SPECIFIC HEATS OF THE PRODUCTS OF COMBUSTION WITH DRY AIR OF A FUEL HAVING THE FORMULA $(CH_2)_x$

[Hydrogen-carbon ratio = 0.168]

Fuel-air ratio	Temperature (°F)	γ	Mean molecular weight	Fuel-air ratio	Temperature (°F)	γ	Mean molecular weight
0.05	2500	1.2713	28.82	0.09	2500	1.2741	27.14
	3500	1.2592	28.79		3500	1.2611	27.12
	4500	1.2521	28.62		4500	1.2537	27.02
	5000	1.2498	28.35		5000	1.2512	26.92
0.06	2500	1.2663	28.84	0.10	2500	1.2790	26.42
	3500	1.2542	28.80		3500	1.2657	26.42
	4500	1.2472	28.62		4500	1.2582	26.34
	5000	1.2449	28.29		5000	1.2557	26.26
0.07	2500	1.2648	28.62	0.11	2500	1.2832	25.80
	3500	1.2526	28.57		3500	1.2697	25.80
	4500	1.2455	28.36		4500	1.2620	25.74
	5000	1.2432	28.04		5000	1.2594	25.67
0.08	2500	1.2691	27.92	0.12	2500	1.2867	25.20
	3500	1.2565	27.87		3500	1.2750	25.20
	4500	1.2493	27.71		4500	1.2653	25.16
	5000	1.2468	27.60		5000	1.2627	25.10

National Advisory Committee
for Aeronautics

TABLE III

PERCENTAGE DISTRIBUTION OF THE SIX TYPES OF PHOTOGRAPHED CYLINDER-GAS VIBRATION TRACES FOR THREE FUEL-AIR-RATIO RANGES AND FOR TESTS USING A SHROUDED AND AN UNSHROUDED INTAKE VALVE

Fuel-air-ratio range	Type of intake valve	Distribution, percent						Number of traces considered
		Type I	Type II	Type III	Type IV	Type V	Type VI	
0.045-0.070	Shrouded	21.2	5.5	41.6	19.1	3.8	8.8	236
	Unshrouded	8.8	1.6	12.0	24.0	.1	53.5	197
0.070-0.095	Shrouded	26.0	14.6	6.1	34.1	9.5	7.7	392
	Unshrouded	7.0	5.2	16.7	31.0	5.2	34.9	191
0.095-0.125	Shrouded	22.0	12.9	6.3	40.3	10.0	8.5	365
	Unshrouded	12.2	5.1	13.3	35.8	5.1	28.5	98

National Advisory Committee
for Aeronautics

TABLE IV

CALCULATED DENSITY-CORRECTION FACTOR FOR THE EQUATION OF STATE FOR A TYPICAL TEST RUN

[Inlet-air temperature, 200° F]

Fuel-air ratio	Density (grams/ml)	b' (ml/gram)	b' × density	PV/RT (a)
0.045	105.7×10^{-4}	1.198	12.6×10^{-3}	1.0128
.055	56.0	1.177	6.6	1.0067
.065	50.6	1.165	5.9	1.0060
.075	55.4	1.164	5.9	1.0060
.085	65.7	1.168	7.7	1.0078
.095	77.4	1.178	9.1	1.0093
.105	89.5	1.193	10.8	1.0110
.115	104.8	1.212	12.7	1.0129
.125	119.3	1.237	14.7	1.0150

[a]Obtained from table XIII, reference 21, p. 51.

TABLE V

CORRECTION FACTOR FOR GAS IMPERFECTIONS IN THE EQUATION FOR THE SPEED OF SOUND

[Products of combustion of $(CH_2)_x$ fuel with dry air; shrouded intake valve; inlet-air temperature, 200° F]

Fuel-air ratio	B_o	A_o	A_o/RT	V $(ft)^3/(lb\text{-}mole)$	$\dfrac{2B_o - A_o(\gamma+1)/\gamma RT}{V}$
0.05	0.806	791×10^3	0.114	71.25	0.0195
.07	.815	825	.097	88.7	.0160
.09	.760	769	.094	62.6	.0211
.115	.720	682	.096	40.0	.0312

National Advisory Committee
for Aeronautics

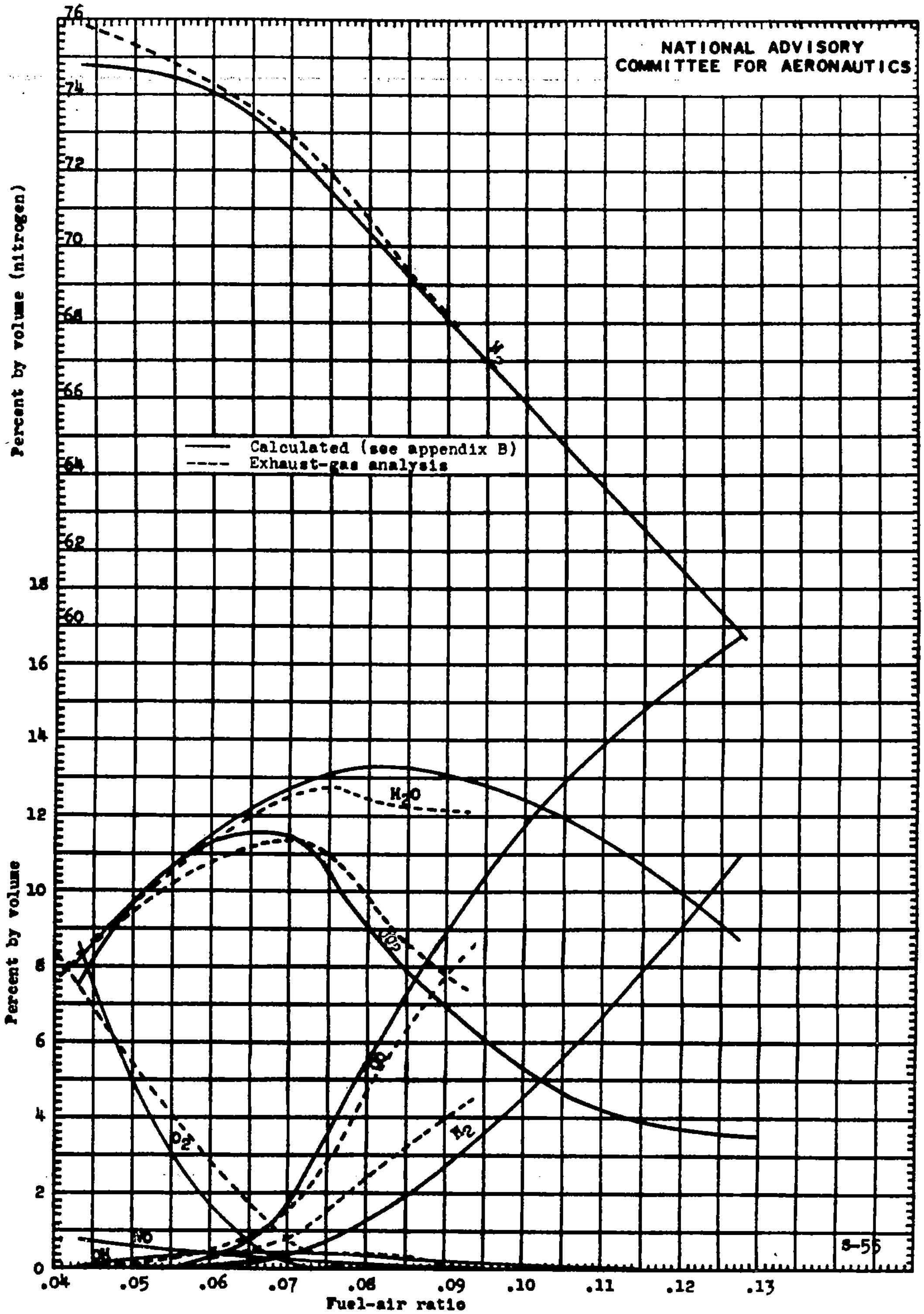

Figure 1. - Variation of the products of combustion with fuel-air ratio. Reactants, dry air and $(CH_2)_x$ fuel. Compositions were calculated by the method of reference 6 for the temperatures indicated by the footnote in table I. Exhaust-gas analysis from reference 16.

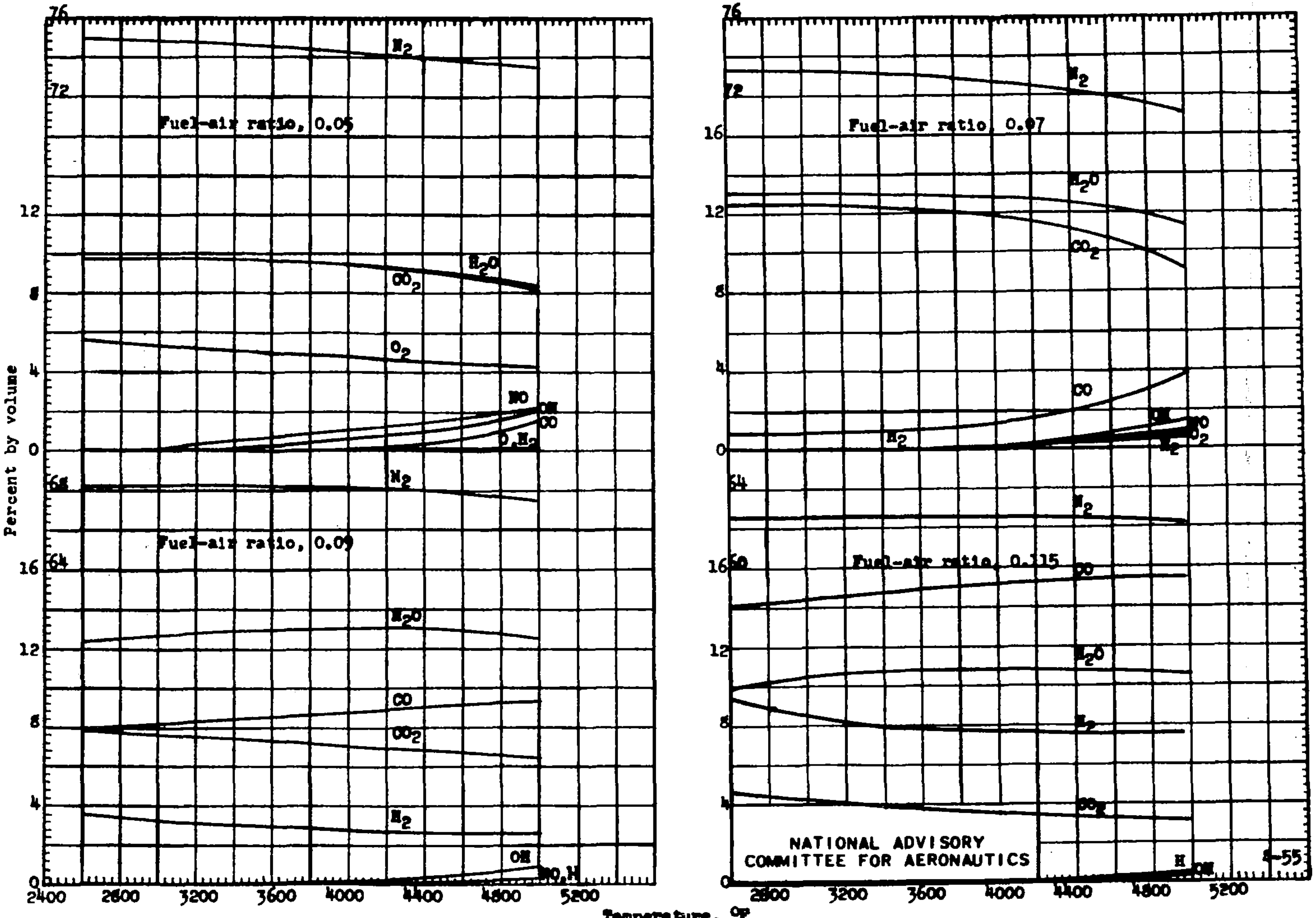

Figure 2. - The effect of temperature on the products of combustion at four fuel-air ratios. Reactants, dry air and $(CH_2)_x$ fuel.

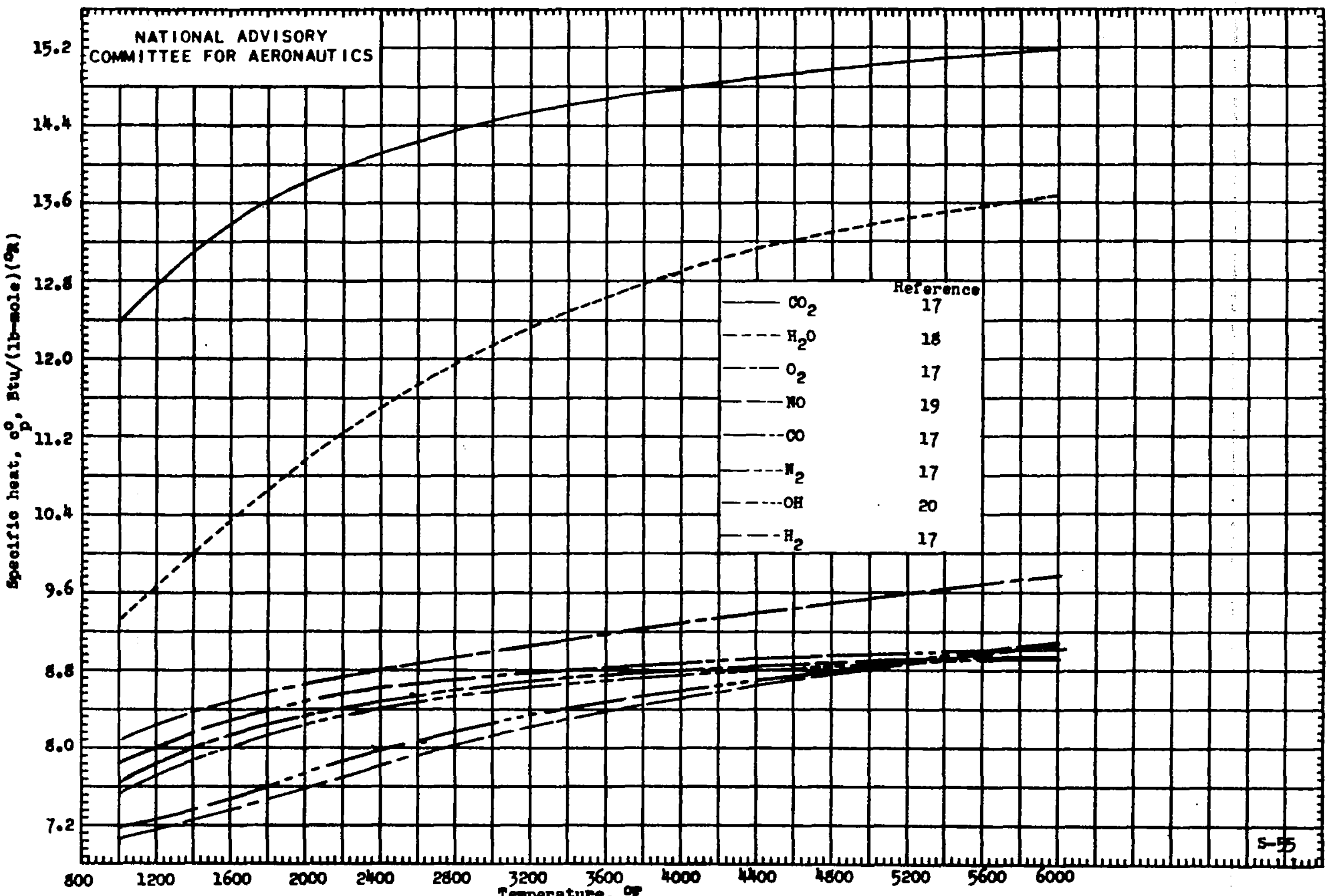

Figure 3. - Temperature variation of the specific heats at zero pressure (c_p^0) of the products of combustion.

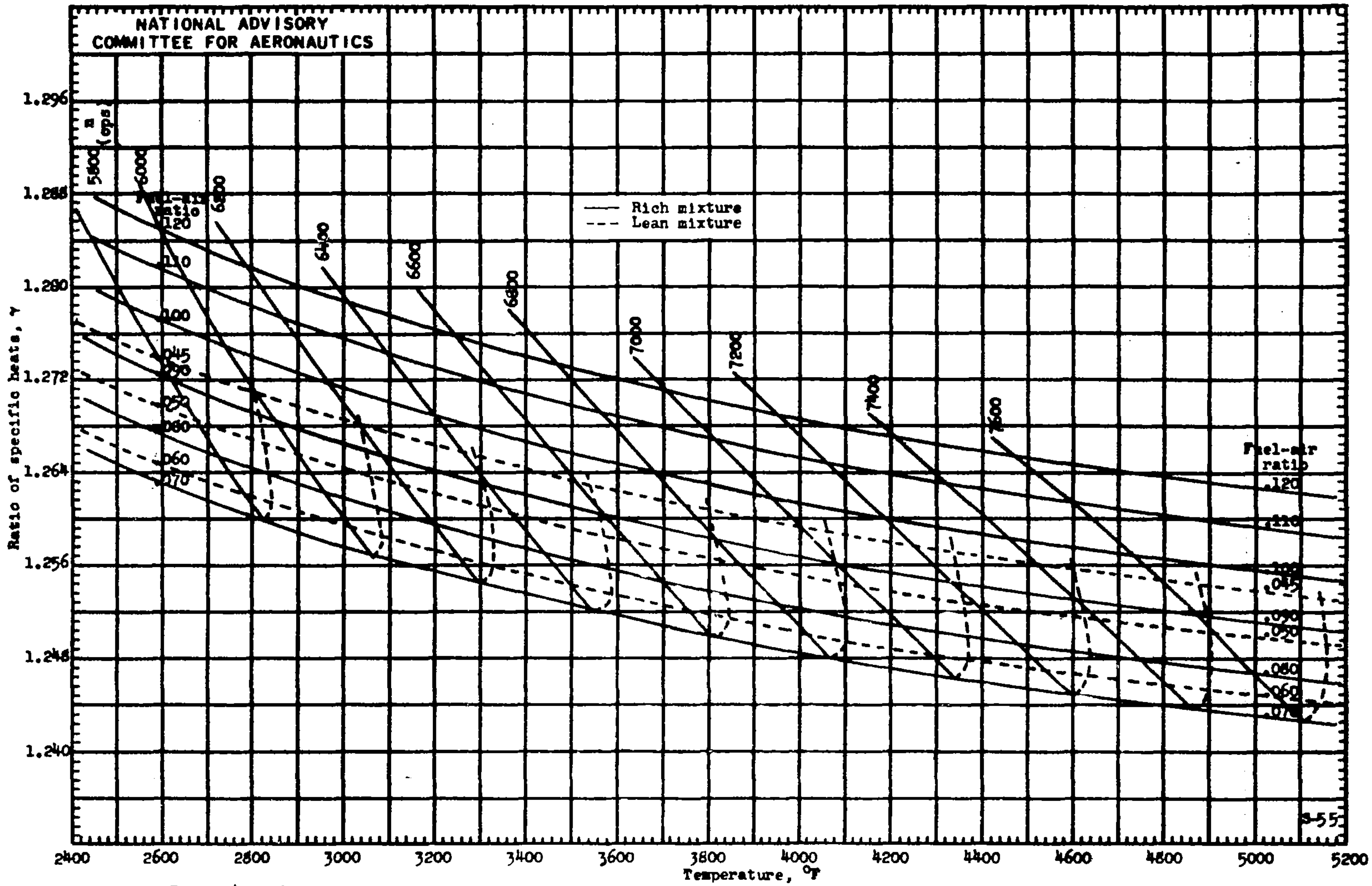

Figure 4. - The variation of the frequency n of the dominant mode of cylinder-gas vibrations and the ratio of specific heats γ of the combustion products with fuel-air ratio and temperature. Flat-ended cylinder; radius, 0.1354 feet; reactants, dry air and $(CH_2)_x$ fuel.

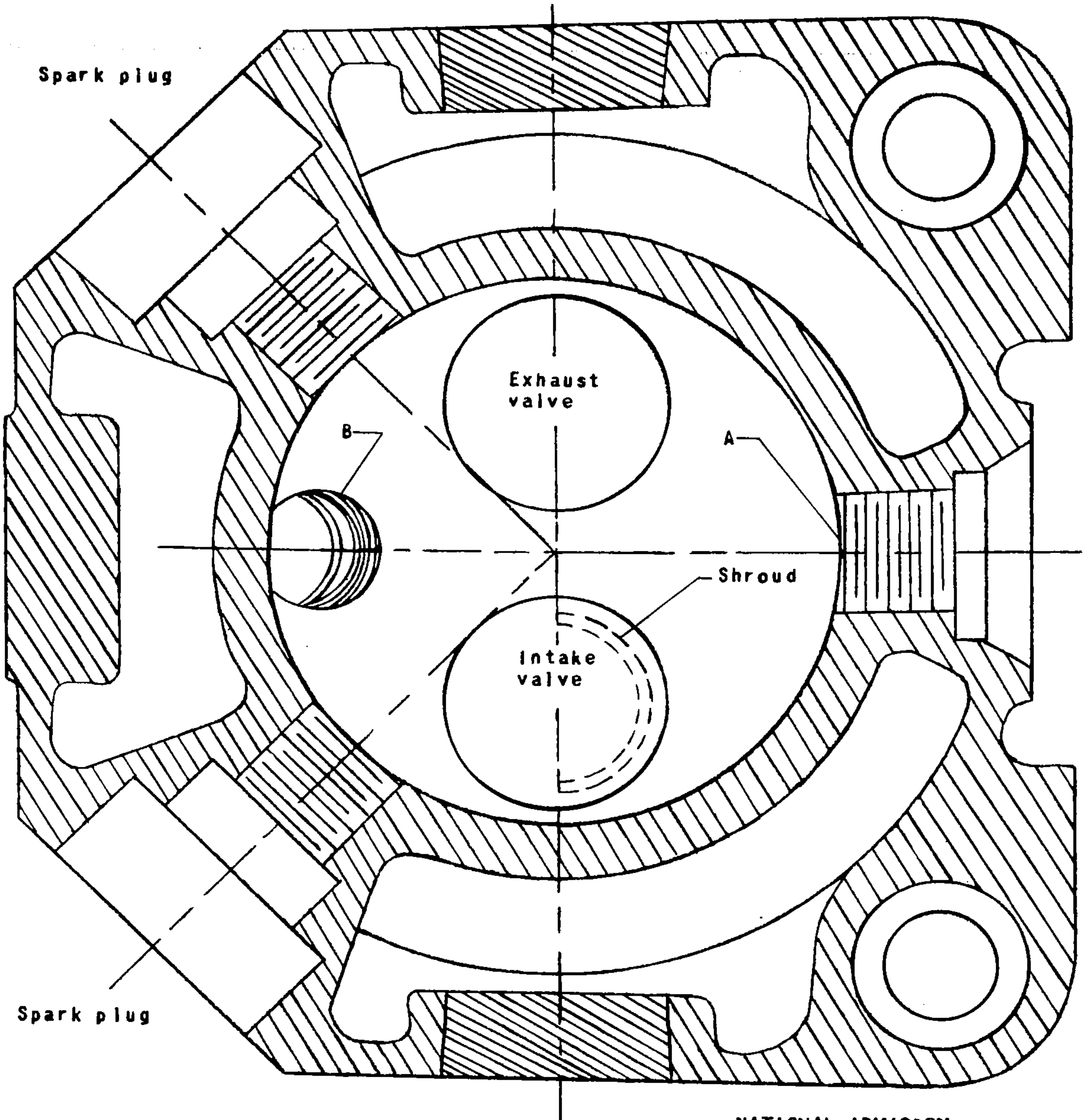

NATIONAL ADVISORY COMMITTEE FOR AERONAUTICS

Figure 5. - Sketch of the CFR cylinder used in this investigation showing the location of the spark-plug holes and the position of the shroud when a shrouded intake valve was used.

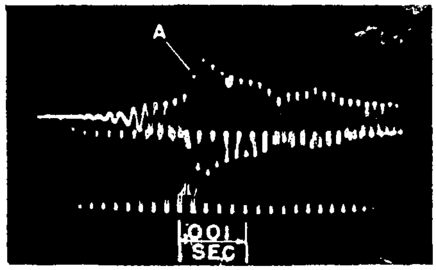

(a) Type I; fuel-air ratio, 0.0795;
frequency, 6818 cycles per second.

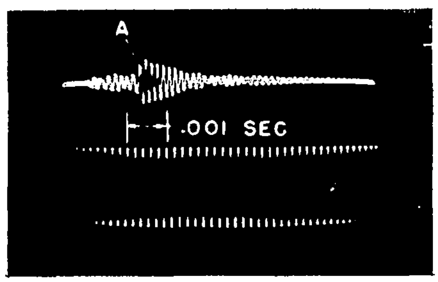

(b) Type I; fuel-air ratio, 0.0643;
frequency, 6750 cycles per second.

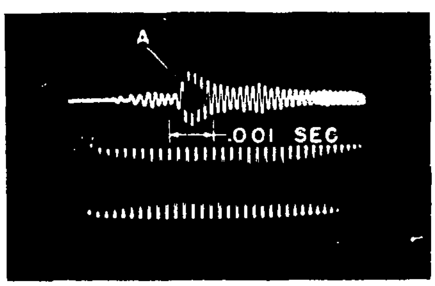

NACA
C-11804
8-10-45

(c) Type I; fuel-air ratio, 0.0853;
frequency, 6897 cycles per second.

Advancing crank angle is toward the right. The indicated frequencies are the average of five vibration cycles following A.

Figure 6. - Photographs of the five types of cylinder gas-vibration traces obtained under knocking conditions. Calibration frequency, 5000 cycles per second; magnetostriction pickup; 4000-10,000 cycles per second band-pass filter; CFR cylinder; shrouded intake valve; inlet-air temperature, 200° F; engine speed, 1800 rpm; compression ratio, 7.0; spark advance, 20° B.T.C.; coolant temperature, 250° F.

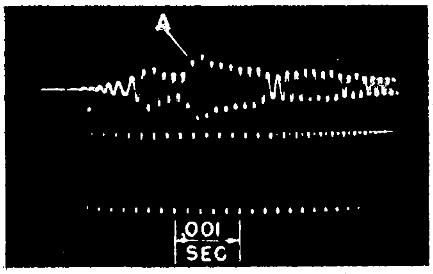

(d) Type II; fuel-air ratio, 0.0795; frequency, 6930 cycles per second.

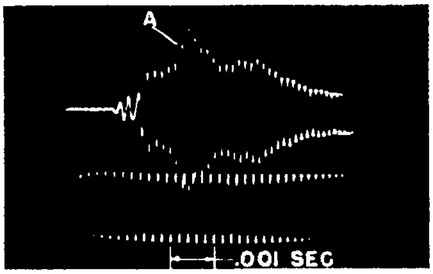

(e) Type II; fuel-air ratio, 0.0853; frequency, 7000 cycles per second.

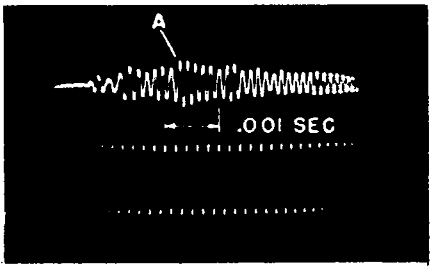

NACA
C-11805
8-10-45

(f) Type II; fuel-air ratio, 0,1052; frequency, 6775 cycles per second.

Advancing crank angle is toward the right. The indicated frequencies are the average of five vibration cycles following A.

Figure 6. - Continued.

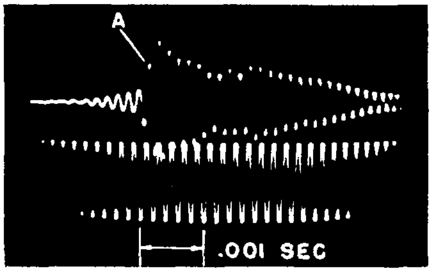

(g) Type III; fuel-air ratio, 0.0472;
frequency, 6240 cycles per second.

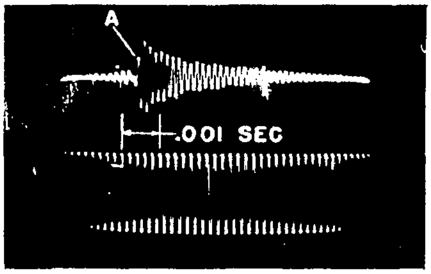

(h) Type III; fuel-air ratio, 0.1152;
frequency, 6430 cycles per second.

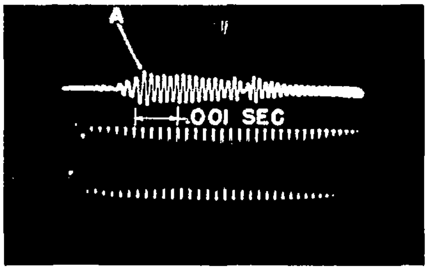

NACA
C-11806
8-10-45

(i) Type IV; fuel-air ratio, 0.0853;
frequency, 6578 cycles per second.

Advancing crank angle is toward the right. The indicated frequencies are the average of five vibration cycles following A.

Figure 6. - Continued.

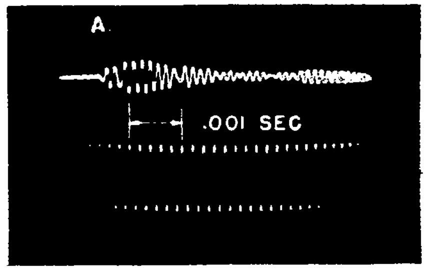

(j) Type IV; fuel-air ratio, 0.1052;
frequency, 6950 cycles per second.

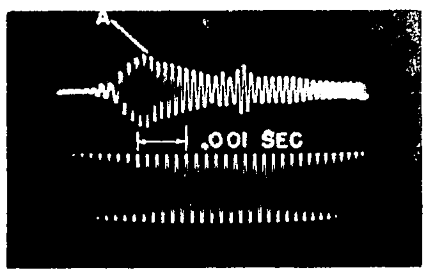

(k) Type IV; fuel-air ratio, 0.1052;
frequency, 6725 cycles per second.

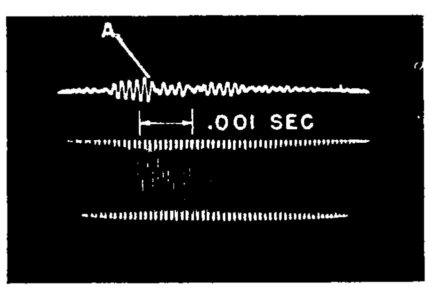

NACA
C-11807
8-10-45

(l) Type V; fuel-air ratio, 0.1152;
frequency, 7490 cycles per second.

Advancing crank angle is toward the right.
The indicated frequencies are the average
of five vibration cycles following A.

Figure 6. - Concluded.

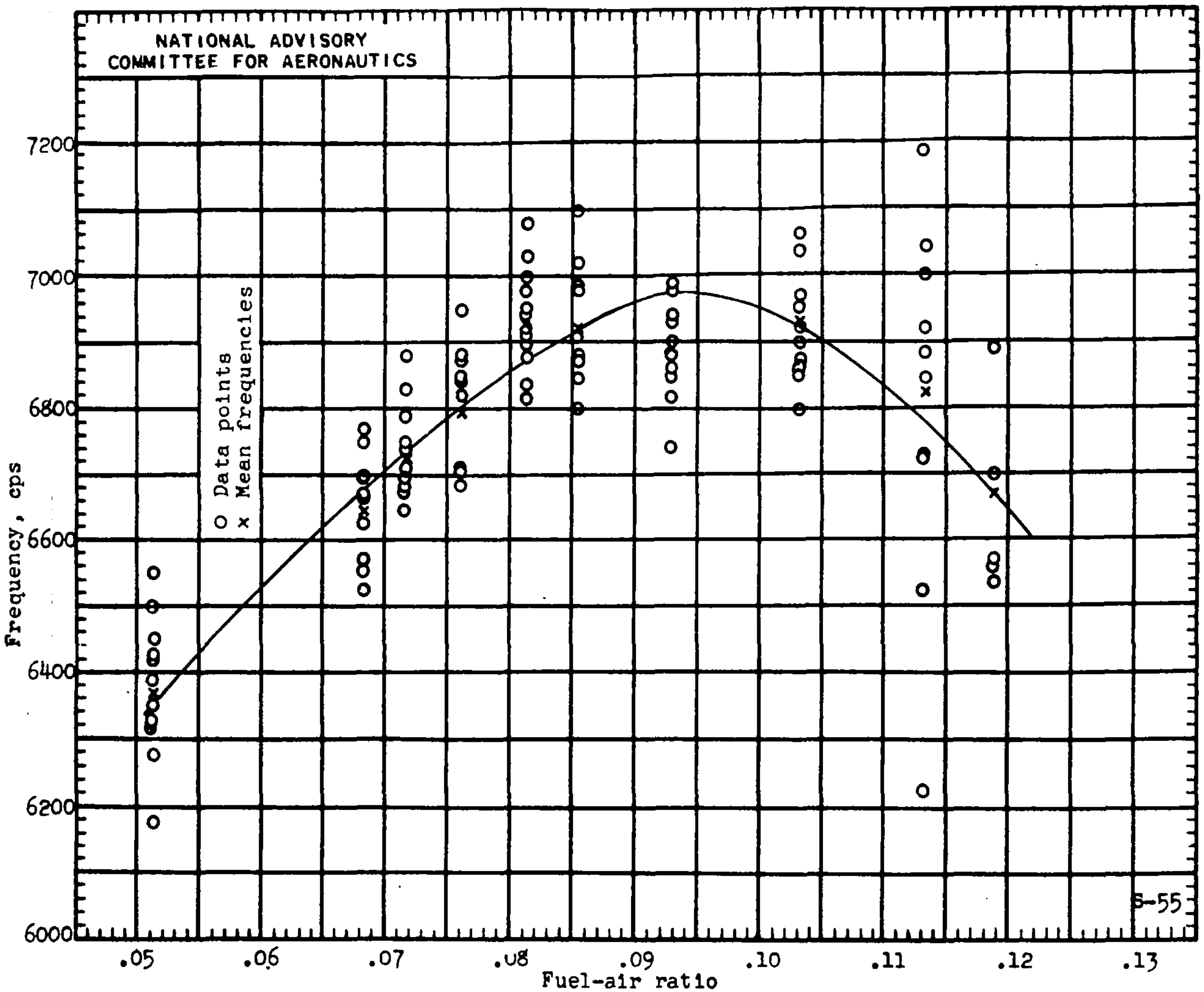

Figure 7. - Distribution of the frequencies of all measurable cylinder gas-vibration traces in a single typical test run. CFR cylinder; shrouded intake valve; inlet-air temperature, 200° F; engine speed, 1800 rpm; compression ratio, 7.0; spark advance, 20° B.T.C.; coolant temperature, 250° F.

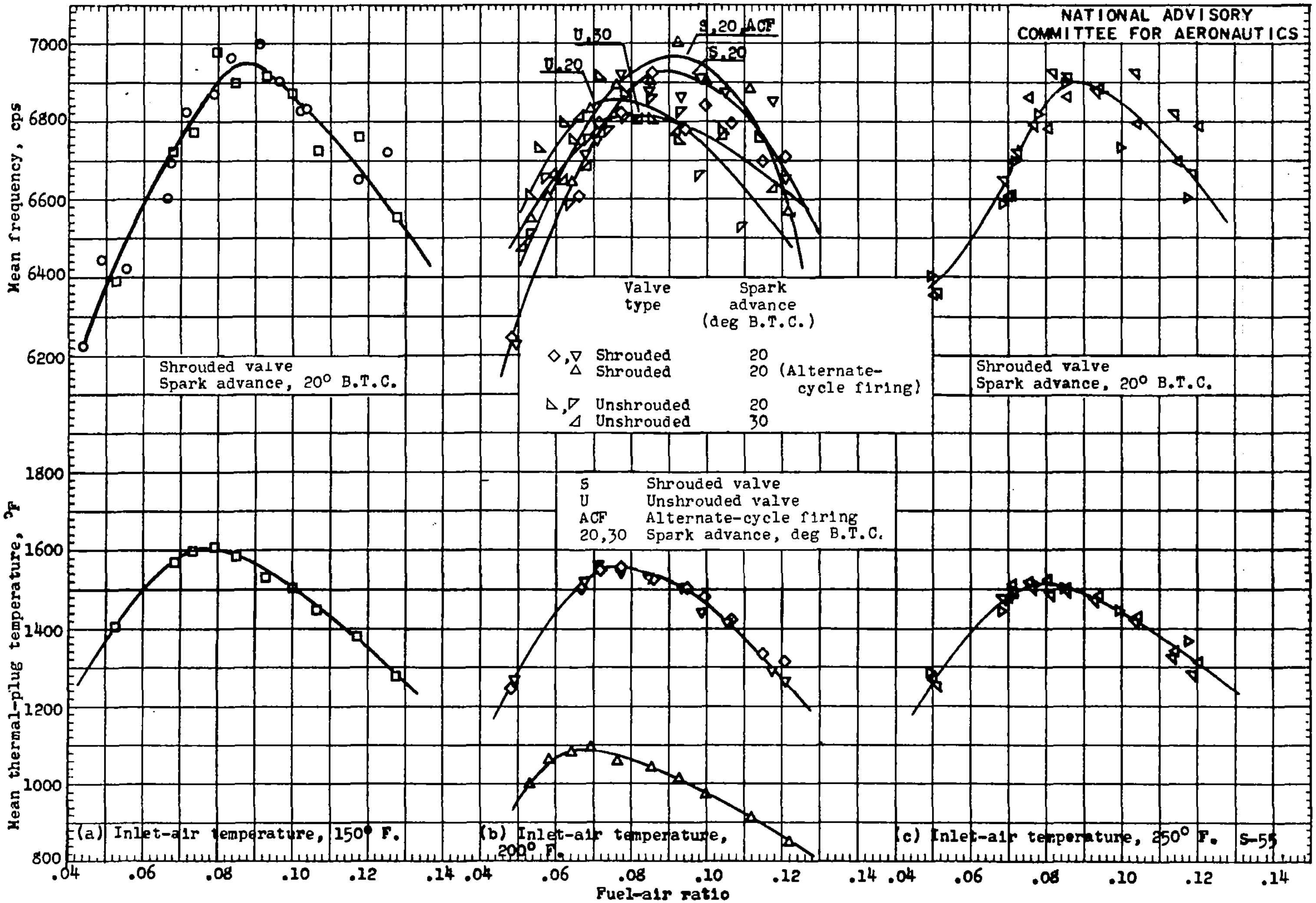

Figure 8. - The variation with fuel-air ratio of the mean cylinder-gas-vibration frequency and the mean cylinder-gas temperature recorded by a platinum to platinum-rhodium thermal plug. CFR cylinder; engine speed, 1800 rpm; compression ratio, 7.0; coolant temperature, 250° F.

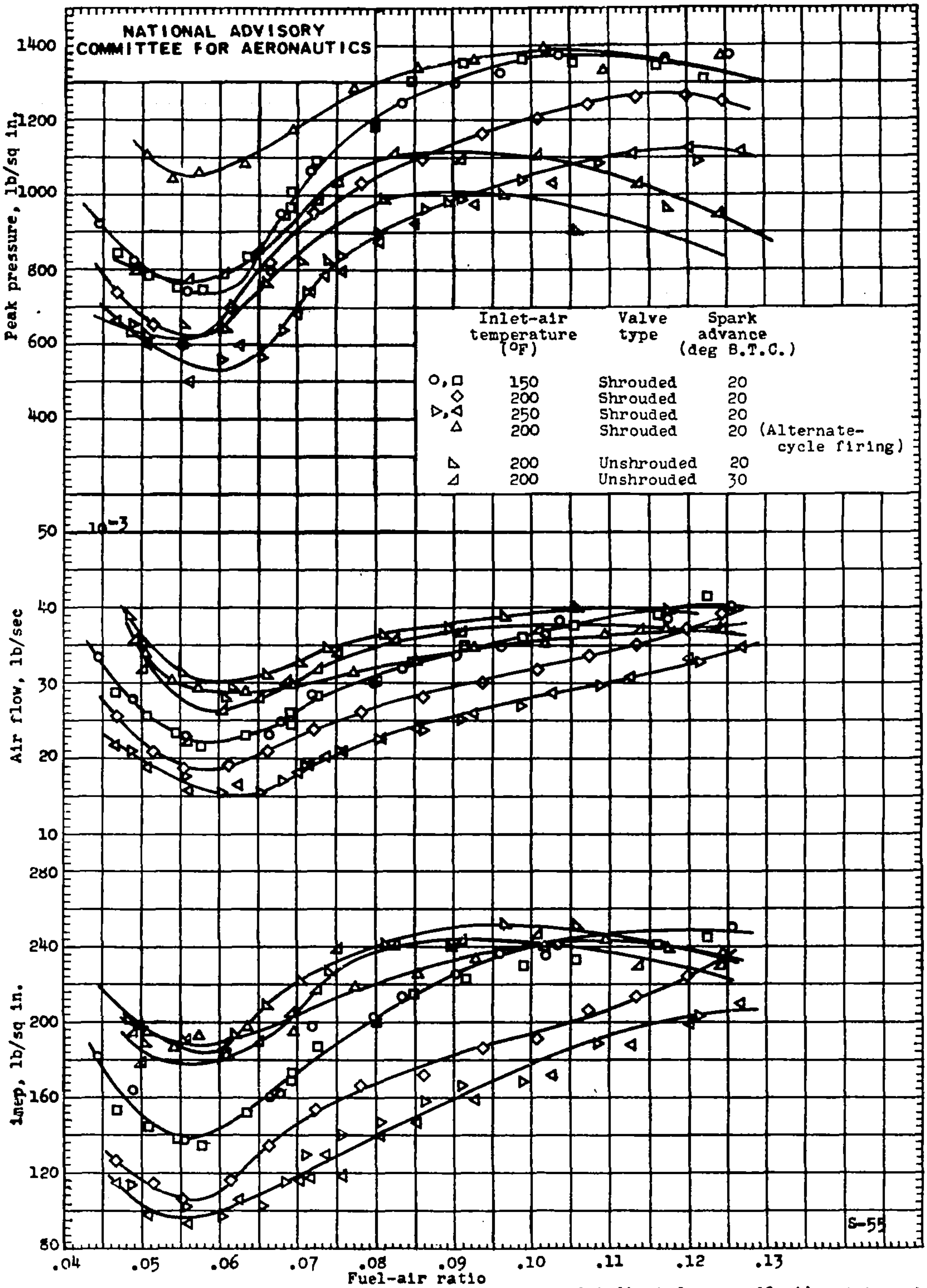

Figure 9. - The variation of peak pressure, air flow, and indicated mean effective pressure with fuel-air ratio for each engine condition for which frequency data were obtained. CFR cylinder; engine speed, 1800 rpm; compression ratio, 7.0; coolant temperature, 250° F.

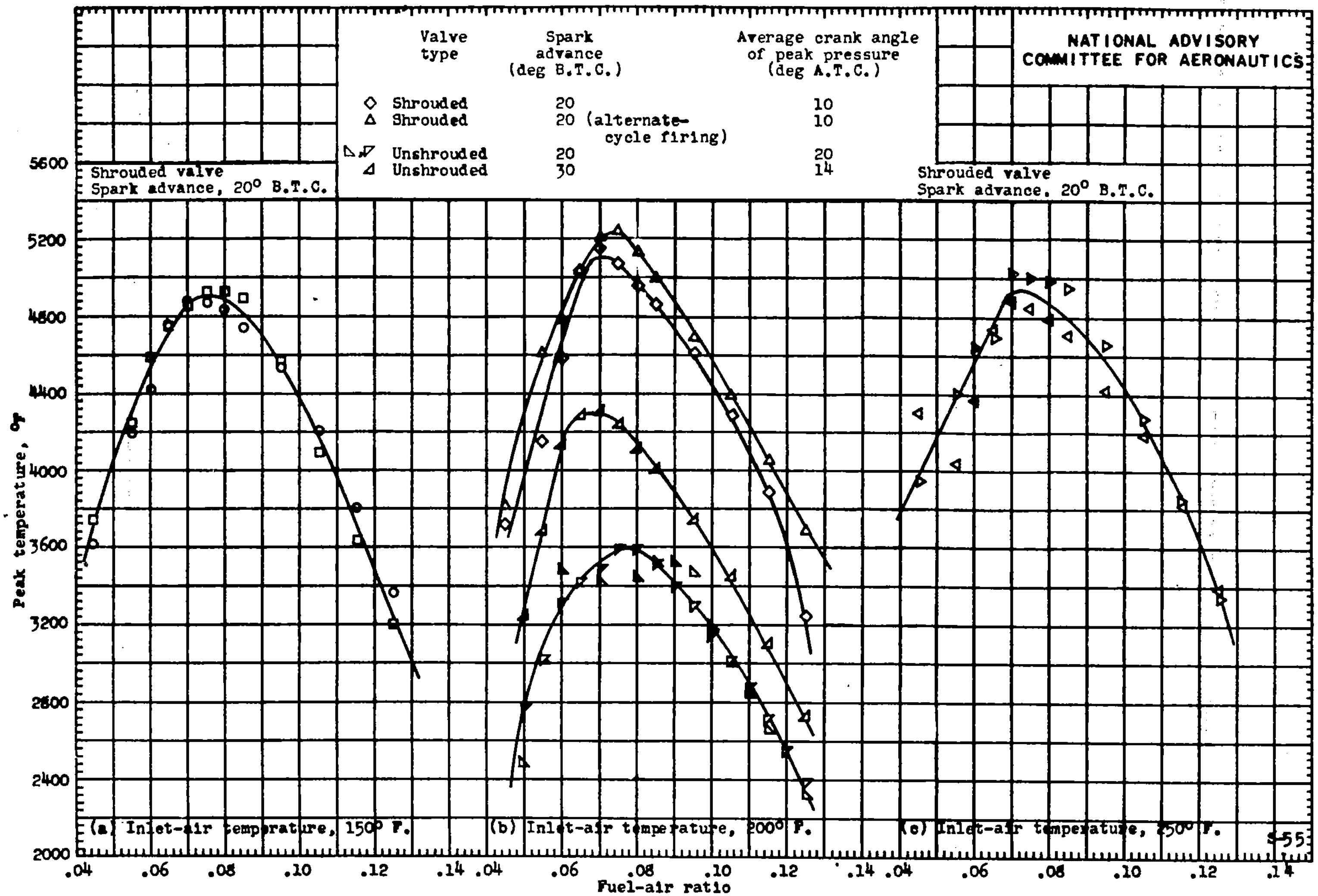

Figure 10. - The variation with fuel-air ratio of the peak temperature calculated from the peak-pressure data of figure 9 for each of the engine conditions for which frequency data were obtained. CFR cylinder; engine speed, 1800 rpm; compression ratio, 7.0; coolant temperature, 250° F.

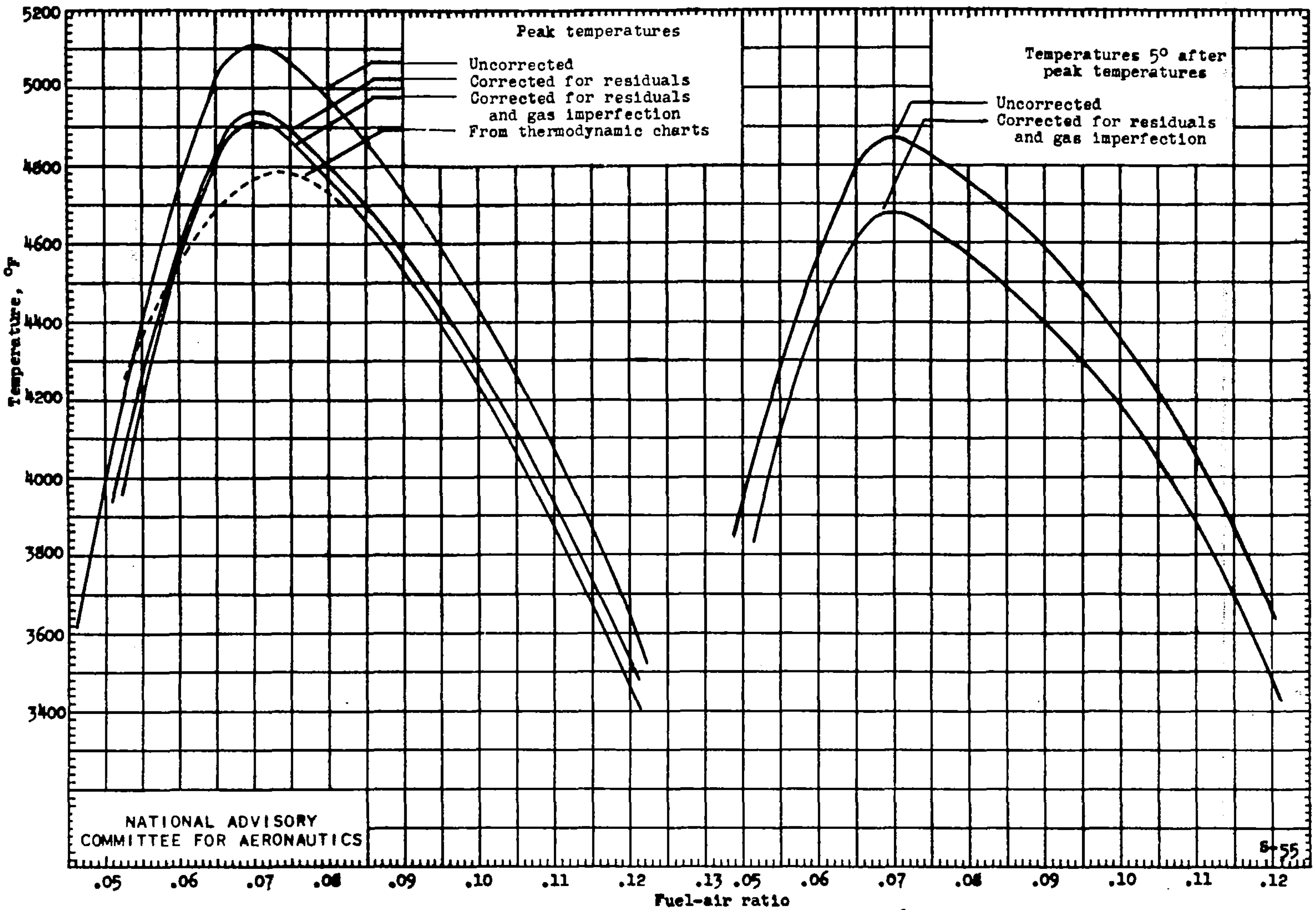

Figure 11. - Effect of corrections on pressure-derived peak temperature and on temperature 5° crank angle after peak pressure. CFR cylinder; shrouded intake valve; inlet-air temperature, 200° F.

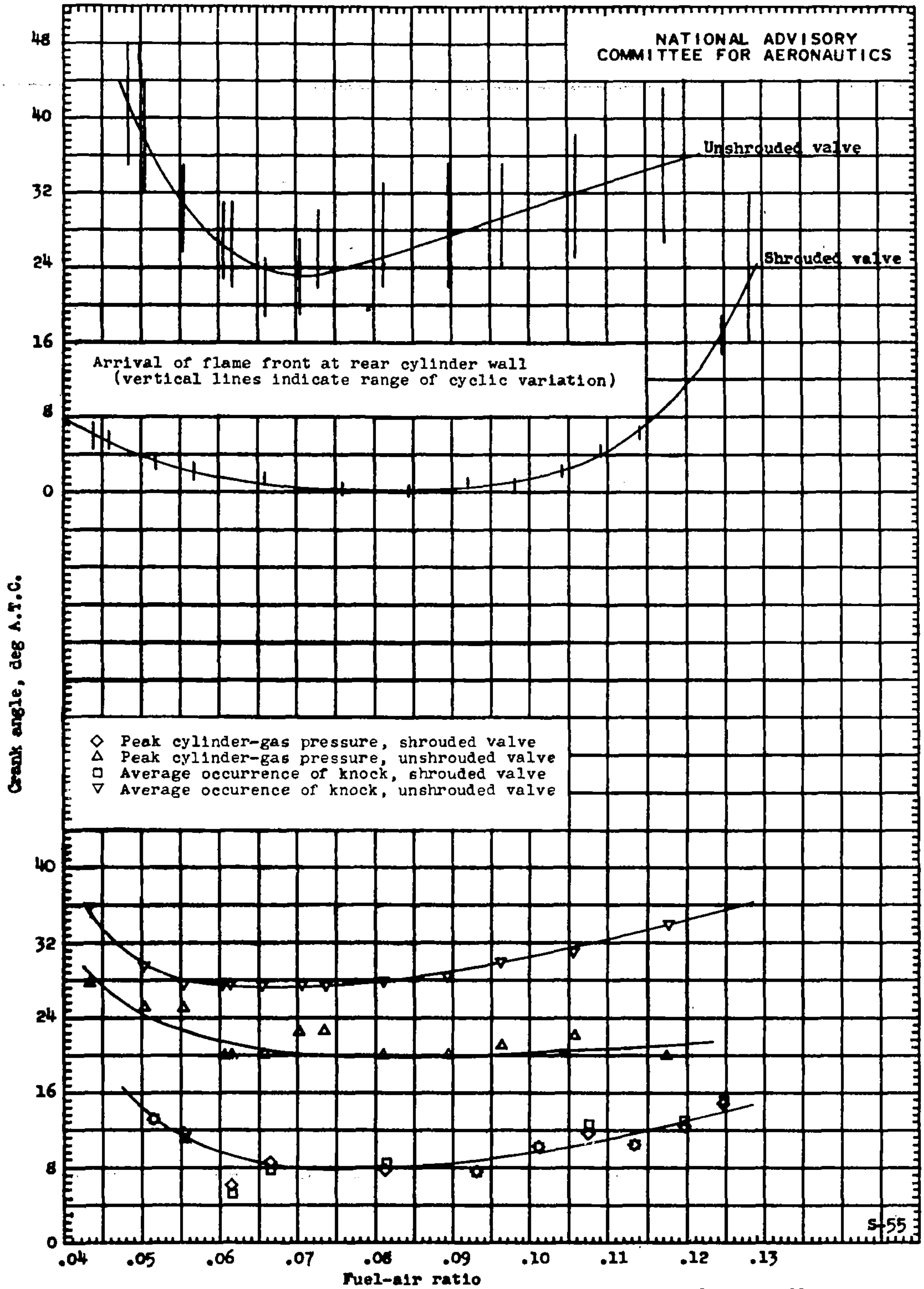

Figure 12. - Crank angle of the arrival of the flame front at the cylinder-wall opposite the spark plugs, the peak pressure, and the average occurrence of knock as functions of fuel-air ratio for tests run with a shrouded and with an unshrouded valve. CFR cylinder; inlet-air temperature, 200° F; engine speed, 1800 rpm; compression ratio, 7.0; spark advance, 20° B.T.C.; coolant temperature, 250° F.

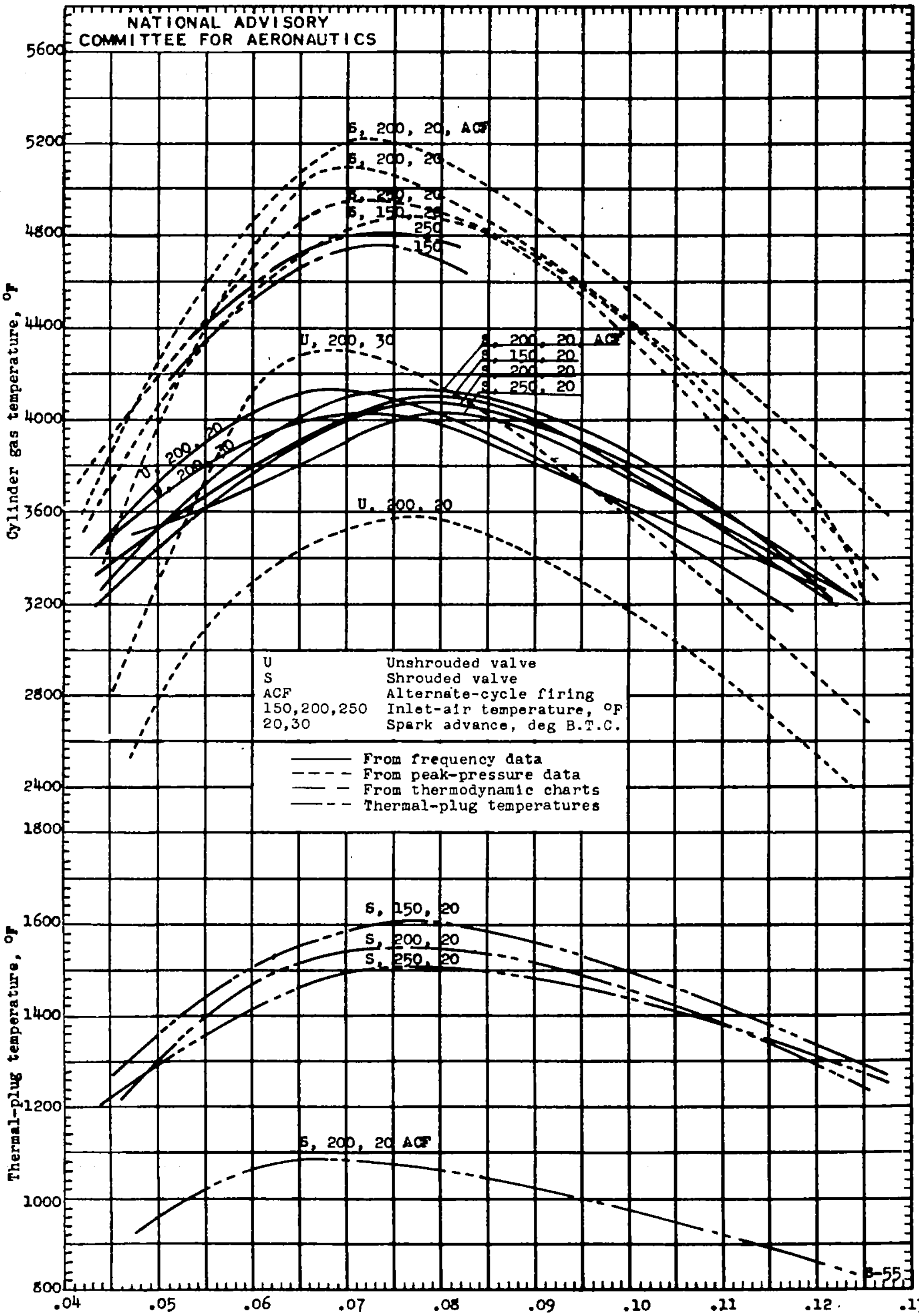

Figure 13. - Comparison of temperatures calculated from cylinder-gas vibration frequencies, uncorrected peak temperatures calculated from peak-pressure curves, peak temperatures obtained from thermodynamic charts, and mean cylinder gas temperatures recorded by a platinum to platinum-rhodium thermal plug.